Spring 5-17-2016

The Cosmic-ray Neutron Probe Method for Estimating Field Scale Soil Water Content: Advances and Applications

William A. Avery
University of Nebraska-Lincoln, avery@huskers.unl.edu

The Cosmic-ray Neutron Probe Method for Estimating Field Scale Soil Water Content: Advances and Applications

by

William Alexander Avery

A THESIS

Presented to the Faculty of

The Graduate College at the University of Nebraska

In Partial Fulfillment of Requirements

For the Degree of Master of Science

Major: Natural Resource Sciences

Under the Supervision of Professor Trenton E. Franz

Lincoln, Nebraska

May, 2016

The Cosmic-ray Neutron Probe Method for Estimating Field Scale Soil Water Content: Advances and Applications

William Alexander Avery, M.S.

University of Nebraska, 2016

Advisor: Trenton E. Franz

The need for accurate, real-time, reliable, and multi-scale soil water content (SWC) monitoring is critical for a multitude of scientific disciplines trying to understand and predict the earth's terrestrial energy, water, and nutrient cycles. One promising technique to help meet this demand is fixed and roving cosmic-ray neutron probes (CRNP). However, the relationship between observed low-energy neutrons and SWC is affected by local soil and vegetation calibration parameters. This effect may be accounted for by a calibrated equation based on local soil type and the amount of standing biomass. However, determining the calibration parameters for this equation is labor and time intensive, thus limiting the full potential of the roving CRNP in large surveys and long transects, or its use in novel environments. In this work, our objective is to develop and test the accuracy of using globally available datasets (clay weight percent, soil bulk density, and soil organic carbon) to support the operability of the CRNP. Here, we develop a 1 km product of soil lattice water over the CONtinental United States (CONUS) using a database of *in-situ* calibration samples and globally available soil taxonomy and soil texture data. We then test the accuracy of the global dataset in the CONUS using comparisons of 61 *in-situ* samples of clay percent (RMSE = 5.45 wt. %, R^2 = 0.68), soil bulk

density (RMSE = 0.173 g/cm^3, R^2 = 0.203), and soil organic carbon (RMSE = 1.47 wt. %, R^2 = 0.175). In addition, we conduct an uncertainty analysis of the global soil calibration parameters using a Monte Carlo error propagation analysis (maximum RSME ~0.035 cm^3/cm^3 at a SWC = 0.40 cm^3/cm^3). Fast growing crops (i.e. maize and soybeans) contribute to the CRNP signal primarily through the water within their biomass and this signal must be minimized for soil moisture retrieval. This was done by using a vegetation index derived from MODIS imagery as a proxy for standing wet biomass (RMSE < 1 kg/m^2). Lastly, we make recommendations to the design and validation of future roving CRNP experiments.

Acknowledgements

This research would not have been successful without funding support from the Robert B. Daugherty Water for Food Institute. My opportunity for a graduate fellowship provided me the capacity to pursue this research and help further the goals of global food security for which the Water for Food Institute is dedicated. Additional financial support has been provided by the NSF EPSCoR FIRST Award, the Cold Regions Research Engineering Laboratory through the Great Plains CESU, and an USGS104b grant. I would like to thank Chase Johnson and Romher Farms for providing access to field sites, Gary Womack and Darin Desilets for support with the rover, and Mark Kuzila for assistance with soil taxonomy. I sincerely appreciate the support and the use of facilities and equipment provided by the Center for Advanced Land Management Information Technologies, School of Natural Resources and data from Carbon Sequestration Program, the University of Nebraska-Lincoln.

I would like to thank my advisor Dr. Trenton Franz. Dr. Franz has been my mentor throughout my graduate degree. Without his guidance, advice, expertise, and friendship this project would never have been successful. My time with Dr. Franz has continued to develop my passion for a career in science and has given me the skills necessary to be successful in that endeavor. It has been a privilege to learn from him.

I would like to thank my committee members: Dr. Andrew Suyker and Dr. Munoz-Arriola for their assistance and guidance in the development of this thesis. Their help was instrumental in all stages of this work. Without the insight and data these professors provided this work would not have been possible. I would like to thank Dr. Timothy Arkebauer, Dr.

Anthony Nguy-Robertson, and Dr. Tiejun Wang. These scientists offered their time, data, advice, and guidance during crucial stages of this projects development. I am grateful for their support and faith. I would also like to thank Catherine Finkenbiner whose work on this project constituted a major contribution without which this work would be incomplete.

Lastly, a special thanks to Dr. Diego Riveros-Iregui. My advisor and mentor during my undergraduate years. The friendship, direction, and academic guidance Dr. Riveros-Iregui gave me originally inspired me to pursue a career in science. Without the opportunities he provided me, I would not be where I am today.

Table of Contents

Table of Figures

Figure 2.6: Propagation of error analysis using Monte Carlo simulations of 100,000 soil parameter datasets of true soil parameters (i.e. soil bulk density, lattice water, soil organic carbon) and perturbed parameters with matching mean differences and covariance matrix between *in-situ* samples and GSDE derived parameters (see Table 2.2). Three error metrics are presented across a range of neutron counts (and thus SWC values). Note that soil bulk density was constrained to 1.2-1.5 g/cm^3, lattice water was constrained from 1-8 wt. %, soil organic carbon was constrained from 0-8 wt. %, and soil water content was constrained from 0.03-0.45 cm^3/cm^3. Simulated and calculated values outside of these bounds were either reset to the minimum or maximum or removed from the Monte Carlo statistics. A minimum threshold of 70% of simulated cases were used to compute error statistics.

Table of Tables

List of Parameters and Abbreviations

Parameter/Abbreviation	Description
N_0	Neutron count rate in a dry soil environment (counts/time)
$N_0(0)$	Instrument specific estimate of N_0 with no standing biomass
f_{WE}	Stoichiometric ratio of H_2O to cellulose, 0.494
θ_{LW}	Soil lattice water (g/g)
θ_{SOC}	Soil organic carbon water equivalent (g/g)
θ_T	Total gravimetric water content (g/g)
θ_p	Soil gravimetric pore water content (g/g)
ρ_b	Dry soil bulk density (g/cm^3)
ρ_w	Density of water, 1 g/cm^3
a_0	Constant, 0.0808
a_1	Constant, 0.3720
a_2	Constant, 0.1150
AWDN	Nebraska Automated Weather Data Network
BWE	Biomass water equivalent (kg/m^2 ~ mm of water/m^2)
CONUS	Continental United States
CRN	Climate Reference Network
CRNP	Cosmic-ray Neutron Probe
GrWDRVI	Green Wide Dynamic Range Vegetation Index
GSDE	Global Soil Dataset
LSM	Land Surface Model
MODIS	Moderate Resolution Imaging Spectroradiometer (NASA)
N	Epithermal corrected neutron count rate (counts/time)
NRCS	Natural Resources Conservation Service
RMSE	Root Mean Squared Error
SCAN	Soil Climate Analysis Network
SDB	Standing dry biomass (kg/m^2 ~ mm of water/m^2)
SMAP	Soil Moisture Active Passive (NASA)

SMOS	Soil Moisture and Ocean Salinity (European Space Agency)
SSURGO	Soil Survey Geographic Database
SWB	Standing wet biomass (kg/m^2 ~ mm of water/m^2)
SWC	Soil Water Content
TC	Soil Total Carbon (g/g)
TIC	Soil Total Inorganic Carbon (g/g)

Chapter 1: Foreword

By the year 2050, over nine billion people are predicted to inhabit the Earth (United Nations, 2015). The monumental task of feeding the projected global population will require a near doubling of grain production (FAO, 2009). As of today, the majority (~2/3) of water consumption by humans is used for agriculture, where approximately half of all global food production comes from irrigated agriculture (Mekonnen et al., 2011). As such, an increase in food demand will put an even greater demand on fresh water resources, particularly an increasing reliance on groundwater (Mekonnen et al., 2011). Food security in the coming decades will require accurate knowledge of existing water resources and the hydrologic cycle for effective water resource management. Global food security is one of the challenges of the 21st century. How we choose to meet this challenge will likely come to redefine our relationship with the environment and with each other. The incorporation of new knowledge and technologies into modern agriculture will play a crucial role in meeting the food and water needs of the coming decades. This thesis illustrates the improvement and potential of one such technology, and a glimpse of the future of precision agriculture.

Chapter 2: Incorporation of Globally Available Datasets into the Cosmic-ray Neutron Probe Method for Estimating Field Scale Soil Water Content

2.1 Introduction

The ability to model and forecast the hydrologic cycle will play a major role in effective water resource management in the coming decades. Currently, most land surface models (LSM) aimed at characterizing the fluxes of water, energy, and nutrients, have relied on either sparse point scale *SWC* monitoring networks (Crow et al. 2012) or remote sensing products with large pixel sizes (~36 km) and shallow penetration depths (e.g., ~ 2-5 cm for SMOS; Kerr et al., 2010 and SMAP Entekhabi et al., 2010). A critical scale gap exists between these methods requiring innovative monitoring strategies (Robinson et al., 2008). Moreover, as LSMs continue to move towards highly refined spatial resolutions of 1 km or less (Wood et al., 2011), the need for accurate and spatially exhaustive *SWC* datasets continues to grow (Beven and Cloke, 2012).

Estimating and monitoring *SWC* at the appropriate spatial and temporal scale for effective incorporation into LSMs has proven to be a difficult task. On one hand, monitoring networks at the regional (e.g., Nebraska Automated Weather Data Network; AWDN, Oklahoma Mesonet) and continental scales (Climate Reference Network; CRN, Soil Climate Analysis Network; SCAN) have continuously recording point sensors. However, these networks have limited spatial coherence due to the nature of point based *SWC* sensors only representing the point at which they are placed, and not the surrounding landscape (Vereecken et al., 2008). Techniques such as temporal stability analysis (Vachaud et al., 1985) can help improve the representativeness of the monitoring networks but require *a priori* spatial information. On the other hand, remote sensing

satellites using passive microwaves can monitor global *SWC* data every few days albeit with large spatial footprints (~36 km, Entekhabi et al., 2010; Kerr et al., 2010). In addition, passive microwaves lack significant penetration depths (~ 2-5 cm Njoku et al., 1996), limiting their effectiveness as a remote sensing input for full root zone coverage in LSMs.

Alternatively, the field of geophysics offers a variety of techniques to help fill the spatial and temporal gaps between point sensors and remote sensing products (Robinson et al., 2008). Bridging this gap requires both novel geophysical techniques and integrated modeling strategies capable of merging both point and remotely sensed data into a unified framework (Binley et al., 2015). One promising geophysical technique to help fill this need is fixed (Desilets et al., 2010, Zreda et al., 2012) and roving cosmic-ray neutron probes (CRNP; Chrisman et al., 2013, Dong et al., 2014), which measures the ambient amount of low-energy neutrons in the air. The low-energy neutrons are highly sensitive to the mass of hydrogen, and thus *SWC*, in the near surface (Zreda et al., 2012). CRNP estimate the area-average *SWC* because neutrons are well mixed within the footprint of the sensor which typically has a radius of ~300 m and depths of ~12-76 cm (Desilets and Zreda 2013, Kohli et al., 2015).

To date, the CRNP method has been mostly used as a fixed system in one location to continuously measure *SWC* as part of a large monitoring network (Zreda et al., 2012, Hawdon et al., 2014). Recent advancements have allowed the CRNP to be used in mobile systems to monitor transects across Hawaii (Desilets et al., 2010), monitor entire basins in southern Arizona (Chrisman et al., 2013), compare against remote sensing products in central Oklahoma (Dong et al., 2014), and monitor ~140 agricultural fields in eastern Nebraska (Franz et al., 2015). In order to accurately estimate *SWC*, the CRNP method relies on a calibration function to convert observed low-energy neutron counts into *SWC* (Desilets et al., 2010, Bogena et al., 2013, see

Sec. 2.2 for full details). The calibration procedure requires site specific sampling of both soil and vegetation data in order to determine the required parameters. While the calibration of a fixed CRNP is fairly standardized (Zreda et al., 2012; Franz et al., 2012; Iwema et al., 2015, Baatz et al., 2015), the heterogeneous nature of soil and vegetation characteristics across a landscape makes the pragmatic calibration of the mobile CRNP a significant challenge. Specifically, the presence of water within vegetation and the soil minerals may alter the shape of the local calibration function and thus accuracy of *SWC*. The need for reliable, accurate, depth-dependent, and localized soil and vegetation spatial information for use in the calibration function is critical in order to fully harness the potential of the CRNP to monitor landscape scale *SWC* across the globe.

The objective of this study is to explore the utility and accuracy of currently available global soil and vegetation datasets (soil organic carbon, soil bulk density, soil clay weight percent, and crop biomass) for use in the calibration function. To accomplish our objective, we aimed to answer the following questions:

1) Can global datasets of soil bulk density, soil organic carbon, and soil clay weight percent be used to in lieu of *in-situ* sampling within reasonable error for use in the CRNP calibration function?

2) Can the use of remotely sensed vegetation products, specifically the Green Wide Dynamic Range Vegetation Index (GrWDRVI) be used to quantify fresh biomass with reasonably low error (< 1 kg/m^2) for use in the CRNP calibration function?

To answer these questions, we tested the accuracy of these datasets against *in-situ* sample datasets of the same parameters. Existing *in-situ* datasets from across the CONUS were then

combined with *in-situ* datasets from eastern Nebraska, which focused on fast growing crops of maize and soybean. Specifically, we tested the accuracy and use of a ~1 km global soil dataset (Shangguan et al., 2014). In addition, we examined the use of the Green Wide Dynamic Range Vegetation Index (*GrWDRVI*, Gitelson, 2004) derived from NASA's MODIS sensor aboard the Terra satellite for use in estimating the amount of fresh crop biomass.

The remainder of this chapter is organized as follows: In the Methods section, the CRNP method is first presented, with emphasis on the integration of the calibration function and soil and vegetation parameters to convert observed low-energy neutron counts into *SWC*. Next, *in-situ* methods for estimating the soil and vegetation calibration parameters are discussed, which is followed by discussions on the soil and vegetation products available globally at ~1 km resolution. In the Results section, we first compare the *in-situ* soil sampling against the global datasets. Next, we develop a 1 km CONUS soil lattice water map using *in-situ* samples. We then compare the *GrWDRVI* against *in-situ* samples from Nebraska to estimate the changes in maize and soybean fresh biomass. Lastly, we present an error propagation analysis investigating the potential uncertainty of using the global soil calibration data vs. local *in-situ* sampling. The paper concludes with a discussion on best practice recommendations for calibrating and validating a roving CRNP experiment.

2.2 Methods

2.2.1 Overview of the Cosmic-ray Neutron Probe

The CRNP estimates area-averaged *SWC* via measuring the intensity of epithermal neutrons near the ground surface (Zreda et al. 2008, 2012). A cascade of neutrons with varying

energy levels are created in the earth's atmosphere when incoming higher energy particles produced within supernovae interact with atmospheric nuclei (Zreda et al., 2012 and Kohli et al., 2015). After fast neutrons are created, they continue to lose energy during numerous collisions with nuclei in air and soil, and become epithermal neutrons (i.e., the neutrons which are primarily measured by the moderated detector). The abundance of hydrogen atoms in the air and soil largely controls the removal rate of epithermal neutrons from the system (Zreda et al. 2012). Water in the near surface soil (i.e. *SWC*) is one of the largest source of hydrogen present in terrestrial systems (McJannet et al. 2014). Thus, relative changes in the intensity of epithermal neutrons are overwhelmingly due to changes in the *SWC*. However, the shape of the calibration function (see section 2.2) is modified by local soil and vegetation parameters (Zreda et al. 2012) reflecting the variation of background hydrogen levels across landscapes.

Using a standard neutron detector with a 2.54 cm layer of plastic, Zreda et al. (2008) first described the support volume the detector measures to be a circle of ~300 m in radius with vertical penetration depths of 12 to 76 cm depending on *SWC*. Recent neutron transport modeling has further refined the footprint area to be a function of atmospheric water vapor, elevation (Desilets and Zreda, 2013), surface heterogeneity (Kohli et al., 2015), vegetation, and *SWC*. Given the large measurement footprint area at tens of hectares, this non-invasive technique is an ideal complement to long-term surface energy balance monitoring around the globe. Currently, there are >200 fixed CRNP (personal communication with Darin Desilets of HydroInnova LLC, Albuquerque, NM) functioning in this capacity around the United States of America (Zreda et al., 2012), Australia (Hawdon et al., 2014), Germany (Baatz et al., 2015), South Africa, China, and the United Kingdom. The real-time *SWC* data provide critical

infrastructure for use in weather forecasting and data assimilation in LSMs (Shuttleworth et al., 2013, Rosolem et al., 2014, Renzullo et al., 2014).

In addition to the fixed CRNP measuring hourly *SWC*, a roving version of the CRNP has been used to reliably measure *SWC* at temporal resolutions as low as 1 minute (Chrisman et al., 2013; Dong et al., 2014) providing the ability to make *SWC* maps over hundreds of square kilometers in a single day. Moreover, Franz et al. (2015) found that a combination of fixed and roving CRNP data in a statistical framework has the ability to form an accurate, real-time, and multiscale monitoring network. With the continued increase in observation spatial scales, the use of *in-situ* sampling in the traditional CRNP calibration procedure is no longer practical, thus requiring the use of alternative available datasets to improve its operability. The remainder of this work will first describe the availability of such global datasets and then test the accuracy of using the datasets in the CNRP calibration function.

2.2.2 The Cosmic-ray Neutron Probe Calibration Function

In order to convert observed epithermal neutron measurements into *SWC*, a series of correction factors and calibration functions have been developed. Zreda (2012) describes in detail the correction factors needed for geomagnetic latitude, changes in incoming high-energy cosmic-ray intensity, and atmospheric pressure. Rosolem et al. (2013) further describes a correction factor for changes in absolute air humidity near the surface. Following these four correction factors, the corrected epithermal neutron counts can be converted into *SWC*. Desilets et al. (2010) proposed the original calibration function (Eq. 1) valid for mass based gravimetric measurements which Bogena et al. (2013) further expanded for volumetric water content. The

calibration function has been successfully tested against direct sampling and point sensor measurements with RMSE < 0.03 cm^3/cm^3 across the globe including arid shrublands in Arizona, USA (Franz et al., 2012), semi-arid forests in Utah, USA (Lv et al., 2014), to humid forests in Germany (Bogena et al., 2013), and across ecosystems in Australia (Hawdon et al., 2014). The original calibration function proposed by Desilets et al., (2010) is:

$$\theta_T = \left(\frac{a_0}{\frac{N}{N_0} - a_1} - a_2 \right) \quad (1)$$

where θ_T (g/g) is the total gravimetric water content, a_0 = 0.0808, a_1= 0.3720, a_2 = 0.1150 (see Desilets et al., (2010) for details), N(counts per time interval) is the aforementioned epithermal corrected neutron count rate, and N_0 (counts per time interval) is the theoretical counting rate at a location with dry silica soils. Zreda et al. (2012) illustrated that:

$$\theta_T = \theta_p + \theta_{LW} + \theta_{SOC} \quad (2)$$

where θ_p (g/g) is the gravimetric pore water content in the soil, θ_{LW} (g/g) is the soil lattice water, and θ_{SOC} (g/g) is the soil organic carbon water equivalent. The volumetric soil water content, *SWC*, (cm^3/cm^3) is found by multiplying θ_p by $\frac{\rho_b}{\rho_w}$, where ρ_b (g/cm^3) is dry soil bulk density and ρ_w = 1 g/cm^3 is the density of water.

To account for effects of time varying above-ground vegetation on the epithermal neutron counts (Franz et al., 2013; Coopersmith et al., 2014), Franz et al. (2015) proposed the following additional correction factor to N_0:

$$N_0(BWE) = m * BWE + N_0(0) \quad (3)$$

where $N_0(0)$ is the instrument specific estimate of N_0 with no standing biomass, BWE is the biomass water equivalent (kg/m^2 ~ mm of water/m^2), and m is the slope of the relationship between N_0 and BWE, determined via *in-situ* calibration datasets. The BWE is further defined as:

$$BWE = SWB - SDB + SDB * f_{WE} \quad (4)$$

where SWB is the standing wet biomass per unit area (kg/m^2 ~ mm of water/m^2), SDB is the standing dry biomass per unit area (kg/m^2 ~ mm of water/m^2), and $f_{WE} = 0.494$ is the stoichiometric ratio of H_2O to organic carbon (assuming organic carbon is cellulose, $C_6H_{10}O_5$). Using nine *in-situ* calibration datasets for maize and soybean crops, Franz et al. (2015) found their roving CRNP had a statistically significant linear relationship between N_0 and BWE yielding $N_0(0) = 518.34$ counts per minute and $m = -4.9506$ (R^2 = 0.515 and p-value = 0.03). We note the coefficients are less suitable for forest canopies given the need for a neutron geometric efficiency factor described further in the supplemental material of Franz et al. (2013). We also refer the reader to Coopersmith et al. (2014) and Baatz et al. (2015) for further discussion of CRNP use in forest canopies.

2.2.3 In-situ Soil and Vegetation Calibration Parameters

The calibration function summarized in equations (1-4) requires depth-average estimates of three soil parameters, θ_{LW}, θ_{SOC}, and ρ_b, and two vegetation parameters SWB and SDB. In order to estimate area-average soil parameters, Zreda et al. (2012) and Franz et al. (2012) recommended averaging 108 individual *in-situ* soil samples from 18 locations (every 60 degrees and radii of 25, 75, 200 m) and six depths (every 5 cm from 0-30 cm) within a CRNP footprint.

In light of recent modeling work (Kohli et al. 2015), this sampling pattern may need to be adjusted to be more representative of encountered conditions (such as shorter sampling distances due to reduced footprint area). Zreda et al. (2012) found that a composite sample of 1 g of material gathered from each of the 108 samples was adequate to estimate θ_{LW} and θ_{SOC}. These composite samples can be analyzed directly for lattice water (g/g), soil total carbon (TC, g/g), and inorganic carbon (TIC, g/g) determined by measuring CO_2 after the sample is acidified (e.g. by Actlabs of Ontario Canada, Analysis Codes: 4E-exploration, 4F-CO2, 4F-C, and 4F-H2O+/-). Franz et al. (2015) reported $\theta_{SOC} = (TC - TIC) * 1.724 * f_{WE}$, where 1.724 is a constant to convert total organic carbon into total organic matter and f_{WE} is given above. To estimate ρ_b at each location, Zreda et al. (2012) used a 30 cm long split tube auger, which contained six 5 cm diameter by 5 cm length rings. All samples were then averaged to get a composite value.

In order to estimate standing wet biomass (*SWB*) and standing dry biomass (*SDB*) in maize and soybeans, Franz et al. (2015) measured average plant density in 1 m^2 quadrats at each of the 18 sampling locations. In a subset of six sites (randomly chosen one radius for each of the six transects) three plants were removed and placed in a paper bag for weighing within two hours (to minimize water loss). The plants were then dried for five days at 70^o C and weighed again. Using the density of plants, wet weight, and dry weight, *SWB* and *SDB* can be determined at each site and averaged across the CRNP footprint.

2.2.4 Global Datasets of Soil Properties

Shangguan et al. (2014) compiled a thirty arc second (~1 km) Global Soil DatasEt (GSDE) with 34 soil parameters in 8 layers (0–0.045, 0.045–0.091, 0.091–0.166, 0.166–0.289,

0.289–0.493, 0.493–0.829, 0.829–1.383, and 1.383–2.296 m). In order to construct an average value relevant to the CRNP, we arithmetically averaged the top four layers in each grid location to form a composite value (~30 cm) over the CONUS. The GSDE contains estimates of soil bulk density and soil organic carbon. In order to construct a map of lattice water, we explored if any relationships existed between clay weight fraction and lattice water following the work of Greacen et al. (1981) using active neutron probe calibration procedures developed for Australian soils. In order to account for variations in chemical and physical weathering on lattice water (Zreda et al., 2012), we further partitioned the analyses based on soil order. A global soil order map with a resolution of five arc minutes (~ 8 km) containing 25 major soil classifications was first uploaded to ArcMap (ESRI, v. 10.2.2) and clipped to the CONUS. The 25 soil classifications were then categorized into 12 major classifications of U.S. soil taxonomy (see Fig. 2.1, personal communication with Prof. M. Kuzila, University of Nebraska-Lincoln).

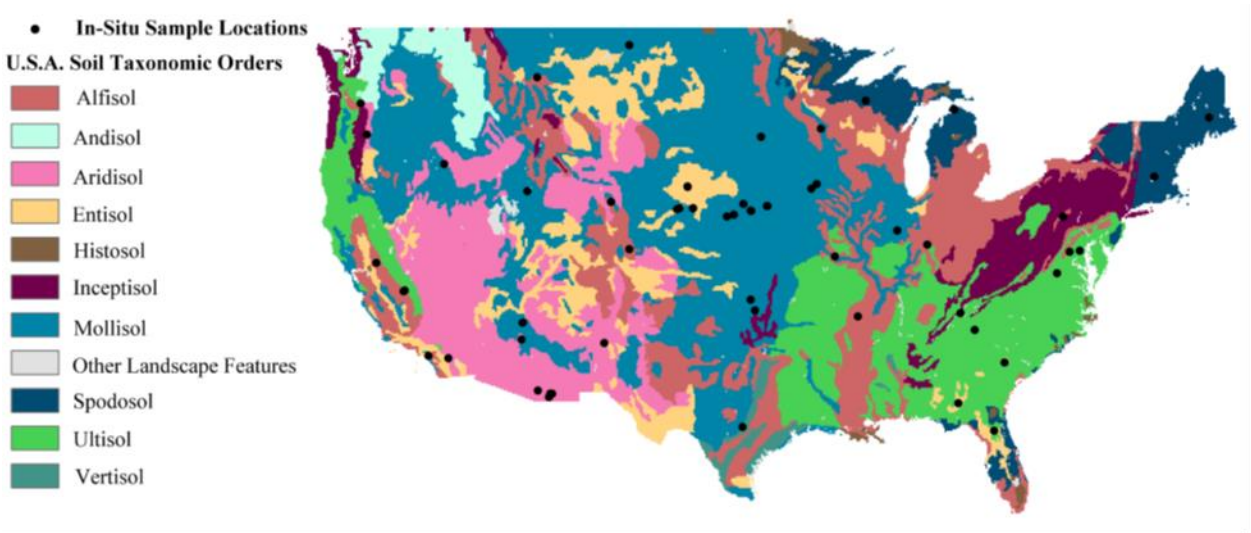

Figure 2.1: Map of soil taxonomic classification map over the Continental United States of America using the twelve USA soil taxonomic orders (data source FAO 2007 and personal communication with M. Kuzila. Note gelisols are not present in the CONUS). Black dots indicate 61 locations where we have *in-situ* composite/average samples for soil bulk density, soil lattice water, soil organic carbon, and clay weight fraction collected over a 12.6 ha circle and averaged over the top 30 cm (Table S2.1).

The reduction from 25 to 12 soil classifications allowed us to generate larger sample sizes for each classification from the available calibration datasets. Using the available lattice water samples from Zreda et al. (2012) and additional samples collected *in-situ* over 2014, we analyzed if any statistically significant relationships existed between GSDE clay weight percent and 61 *in-situ* lattice water samples for each of the US soil orders (Table S2.1). We note that this procedure could be used globally if *in-situ* lattice water samples were available for all 25 soil taxonomic groups. From these relationships, a map of the CONUS lattice water weight percent was developed by using either the mean value of the *in-situ* lattice water or the linear relationships between clay weight percent (from the GSDE) and the lattice water *in-situ* samples. Additionally, *in-situ* samples of soil organic carbon, bulk density, clay weight percent, and lattice water were compared against the same parameters derived from the GSDE.

2.2.5 Global Datasets of Vegetation Properties

In order to estimate *SWB* and *SDB*, we downloaded remotely sensed 500 m MODIS reflectance data from NASA's Terra satellite (http://earthexplorer.usgs.gov/). To calibrate and validate the *in-situ* vegetation data to the remotely sensed vegetation estimates, we sampled two different agricultural areas in eastern Nebraska. The MODIS reflectance data were used to generate various vegetation indices (see detailed information below), and then calibrated against historical biomass data (2003-2013) from 3 fields near Mead, NE. Each field is part of the AmeriFlux network (http://ameriflux.ornl.gov/) with data going back to 2001 (site description given in Suyker et al., 2005). Each field is approximately 65 ha. Field 1 (Mead Irrigated/US-Ne1, 41.1650°, -96.4766°) is irrigated with continuous maize. Field 2 (Mead Irrigated Rotation/US-Ne2, 41.1649°, -96.4701°) is irrigated with a rotation of maize and soybean. Field 3 (Mead Rainfed/US-Ne3, 41.1797°, -96.4396°) is rainfed with a rotation of maize and soybean. At these three fields, destructive biomass samples were collected approximately every two weeks at 6 different locations in the field, typically consisting of 30-35 individual plants per sampling bout. From the destructive sampling bouts, we were able to compute *SWB* and *SDB*. The sites, with their long sampling records consisting of both rainfed and irrigated soybean and maize, are an ideal location for calibrating the remote sensing reflectance data and vegetation indices. In order to validate the derived vegetation index and coefficients from the above mentioned three sites, we used 4 bouts of destructive biomass sampling at two fields (each approx. 65 ha.) during 2014 near Waco, NE (Franz et al. 2015). The fields were irrigated maize (40.9482°, -97.4875°) and irrigated soybean (40.9338°, -97.4587°). *SWB* and *SDB* were collected following the protocol described in section 2.3.

A total of 924 MODIS images over the growing seasons (May to October) between 2003 and 2014 were downloaded for calibration and validation of the corresponding destructive biomass samples at the five field sites in central and eastern Nebraska (note: MODIS images from the closest date to *in-situ* sampling were used with up to a 4 day offset). Using the Python Integrated Development Environment (v. 2.7.8) built into ArcGIS (v. ESRI, v. 10.2.2), we extracted the MODIS reflectance data in the green and near-infrared electromagnetic spectrum range. Next, we removed any pixels that were skewed by incidental cloud cover (Nguy-Robertson & Gitelson, 2015). The resulting data were then transformed from separate reflectance images into the Green Wide Dynamic Range Vegetation Index (*GrWDRVI*; Gietelson, 2004):

$$GrWDRVI = \frac{(0.1 * Near\ Infrared - Green)}{(0.1 * Near\ Infrared + Green)} \quad (5)$$

where near-infrared light (MODIS band 2) has wavelength between 841 and 876 nm and green light (MODIS band 4) has wavelength between 545 and 565 nm. The *GrWDRVI* has been shown to have better correlations with observed *in-situ* biomass as compared to other vegetation indices such as NDVI (Nguy-Robertson et al., 2012; Nguy-Robertson & Gitelson, 2015). We then investigated if any relationships existed between *GrWDRVI* and *SWB* and *SDB*.

2.2.6 Error Propagation Analysis of GSDE Soil Properties

We used a Monte Carlo analysis to estimate the expected uncertainty if the GSDE parameters were used instead of *in-situ* estimates. The statistical metrics of root mean square error (RMSE), mean absolute error (MAE), and bias were used to describe the error propagation in the Monte Carlo simulation experiment. Using the 61 CONUS *in-situ* samples and the GSDE soil properties, we estimated the mean difference and the covariance matrix for θ_{LW}, θ_{SOC}, and

ρ_b. Using these data, we simulated 100,000 realizations of the "true" (i.e. from the *in-situ* sampling) and perturbed soil properties using a multivariate normal distribution. Using a range of observed neutron counts and solving equations (1-2) with the true and perturbed soil properties, we also estimated the true and perturbed *SWC*. In order to provide realistic constraints on the error propagation results, we assumed soil bulk density was constrained between 1.2-1.5 g/cm^3, lattice water between 1-8 wt. %, soil organic carbon between 0-8 wt. %, and *SWC* between 0.03-0.45 cm^3/cm^3. Simulated and calculated values outside of these bounds were either reset to the minimum or maximum value or removed from the Monte Carlo statistics. A minimum threshold of 70% of simulated cases was used to compute all error statistics for each case. We note that the effects of growing biomass were not included here given the lack of available calibration datasets at all sites, but could be incorporated in future work following a similar methodology.

2.3 Results

2.3.1 Comparison of In-situ and Global Soil Calibration Parameters

The comparisons between observed clay weight percent, soil bulk density, soil organic carbon and the GSDE values are summarized in Table S2.1 and Figure 2.2 a, b, c for the 61 sampling sites within the CONUS. Other than 1 outlier (south central Texas, 29.9492º, -97.9966º, which is located on the border between vertisols and alfisol soils), the comparison between the mean observed and GSDE clay weight percent (of sites that had clay weight percent) behaved well excluding one outlier (RMSE = 5.45 wt. %, R^2 = 0.68) considering the difference in scale and methods. The comparisons between soil bulk density (RMSE = 0.173

g/cm^3, R^2 = 0.203) and soil organic carbon as it was during the various 2011-2014 sampling campaigns, (RMSE = 1.47 wt. %, R^2 = 0.175) generally followed the same positive trend.

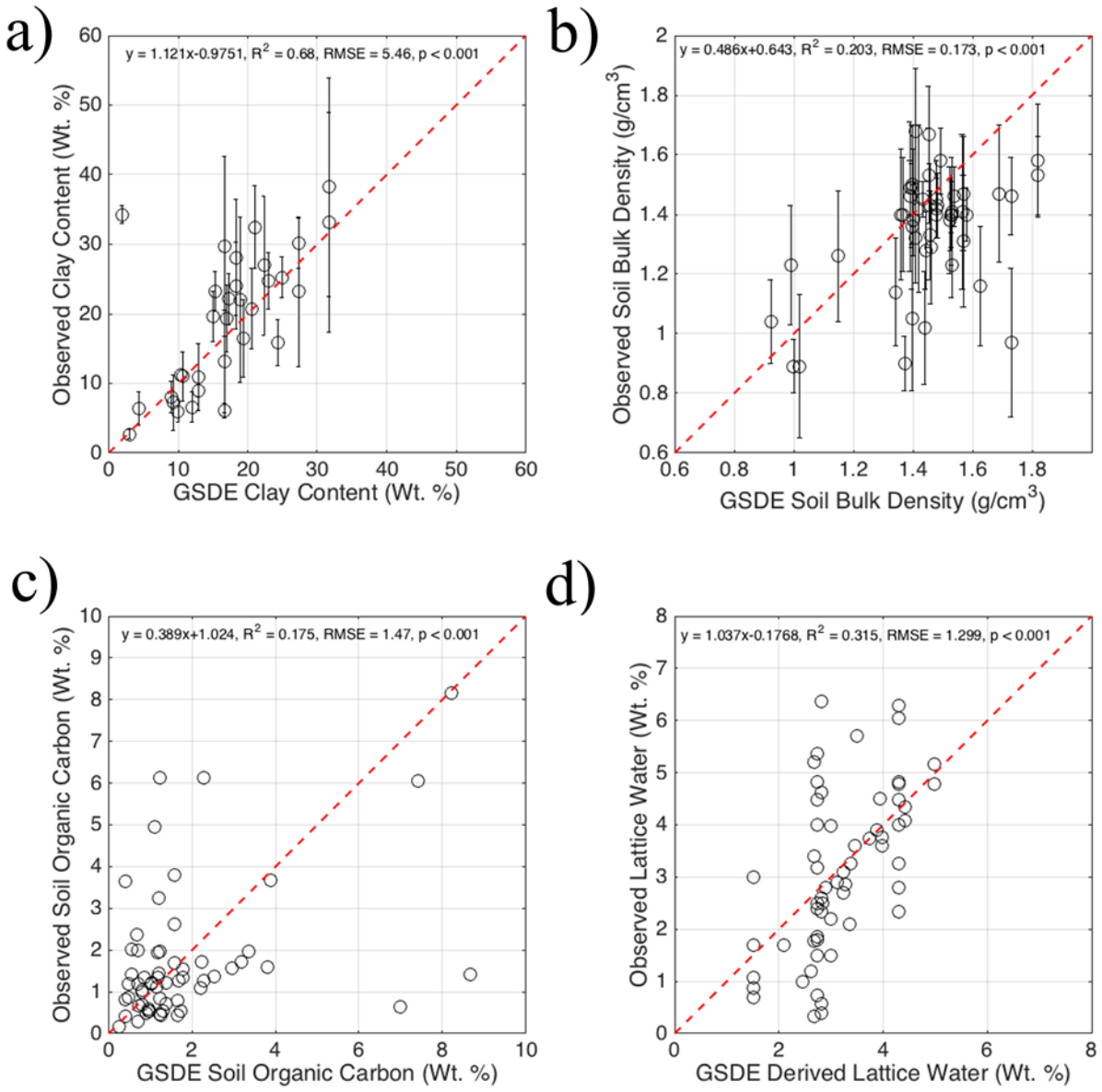

Figure 2.2: Comparison between 61 *in-situ* composite sample and GSDE value from the closest pixel for a) clay weight percent b) soil bulk density, and c) soil organic carbon. d) Comparison between *in-situ* lattice water and derived values using GSDE clay weight fraction and soil taxonomic orders. See Table 2.1 for summary of data by taxonomic group, Table S2.1 for raw data, and Table 2.2 for statistical summary of differences between *in-situ* and GSDE product. Note error bars denote +/- 1 standard deviation.

In order to construct a map of the CONUS lattice water, we investigated if any significant relationships existed between GSDE clay wt. % and observed lattice water for each US soil taxonomic group (Table 2.1) following the relationships described from observations in Australian soils (Greacen, 1981). We found that a significant linear relationship existed between clay wt. % and lattice water for all 61 sites ($R^2 = 0.183$, p value <0.001). However, after partitioning the sites into soil taxonomic groups, only the mollisol taxonomic group yielded a statistically significant relationship ($R^2 = 0.539$, p value <0.001). Therefore, in order to construct a CONUS lattice water map, we used the mean values for six taxonomic groups and neglected the remaining five taxonomic groups due to an inadequate number of samples (Figure 2.3). Figure 2.2d illustrates the comparison between the derived and observed lattice water for the 61 CONUS sites (RMSE = 1.299 wt. %, $R^2 = 0.315$). Table S2.1 summarizes the observed and GSDE values for all 61 sites and Table 2.2 summarizes the mean difference and covariance matrix between the *in-situ* values and GSDE values. The mean difference and covariance differences were used in the error propagation analysis described in section 2.6 and 3.3. We note that each of the mean differences followed a normal distribution (see Table S2.1 for *in-situ* and GSDE values).

USA Soil Taxonomic Group	Mean Lattice Water (Wt. %)	Std. Lattice Water (Wt. %)	Number of Samples	Linear Regression Slope	Linear Regression Intercept	Linear Regression R^2	Linear Regression p value	GSDE Derived CONUS Lattice Water Product
Alfisol	4.31	1.36	9	6.09	-0.11	0.086	0.44330	Mean
Andisol	NA	NA	NA	NA	NA	NA	NA	NA
Aridisol	2.73	1.36	10	4.82	-0.15	0.095	0.38607	Mean
Entisol	1.47	0.93	5	2.48	-0.14	0.233	0.41064	Mean
Gelisol	NA	NA	NA	NA	NA	NA	NA	NA
Histosol	NA	NA	NA	NA	NA	NA	NA	NA
Inceptisol	4.98	0.28	2	NA	NA	NA	NA	Mean
Mollisol	3.18	1.22	24	1.03	0.11	0.539	0.00004	Linear
Oxisol	NA	NA	NA	NA	NA	NA	NA	NA
Spodosol	2.68	2.10	4	3.45	-0.11	0.020	0.85919	Mean
Ultisol	2.82	2.33	6	0.28	0.20	0.229	0.33672	Mean
Vertisol	5.18	NA	1	NA	NA	NA	NA	NA
ALL	3.16	1.58	61	1.68	0.09	0.183	0.00066	NA

Table 2.1: Summary of mean, standard deviation of *in-situ* lattice water samples organized by USA soil taxonomic groups. The table also summarizes a linear regression analysis using the GSDE clay percent and *in-situ* sample. The last column indicates how the 1 km CONUS lattice water map was generated. Note NA stands for not applicable because of a lack of data.

	Bulk Density (g/cm^3)	Lattice Water (Wt. %)	Organic Carbon (Wt. %)
Mean Difference of in-situ value - GSDE value	-0.10035	-0.05789	-0.07077
Covariance matrix of in-situ value - GSDE value			
	Bulk Density (g/cm3)	**Lattice Water (Wt. %)**	**Organic Carbon (Wt. %)**
Bulk Density (g/cm^3)	0.0386	-0.0567	-0.2077
Lattice Water (Wt. %)		1.6745	0.3624
Organic Carbon (Wt. %)			3.5810

Table 2.2: Summary of mean difference between *in-situ* samples and GSDE values (Figure 2.3) for bulk density, lattice water and organic carbon. Bottom) Summary of covariance matrix of difference between *in-situ* values and GSDE values. The mean difference and covariance data were used in an error propagation analysis illustrated in Figure 2.6.

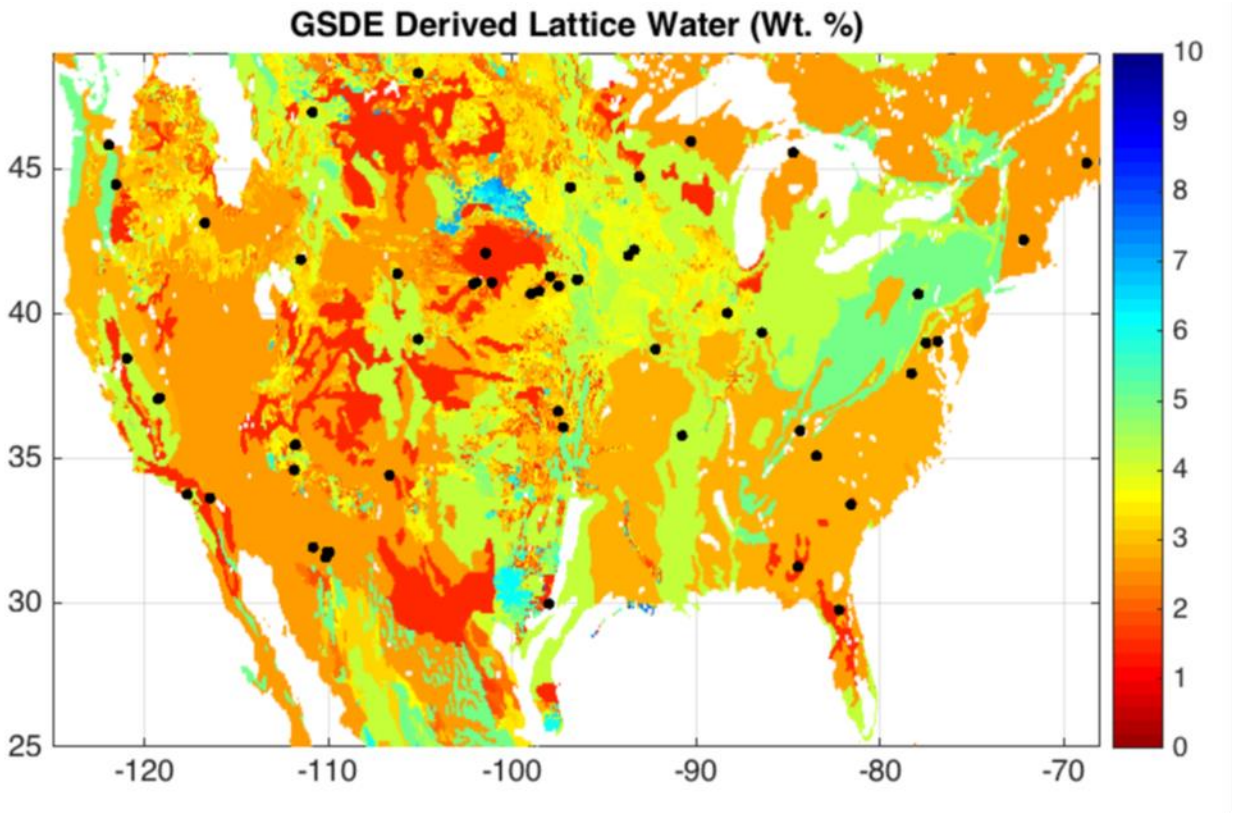

Figure 2.3: Derived 1 km resolution lattice water weight percent map using the GSDE clay percent and regression analyses organized by soil taxonomic classification. See Table 2.1 for estimates of the mean, standard deviation, and linear regression vs. clay percent organized by taxonomic group. Black dots indicate 61 locations where we have *in-situ* composite/average samples for soil bulk density, soil lattice water, soil organic carbon, and clay weight fraction collected over a 12.6 ha circle and averaged over the top 30 cm (Table S2.1). Missing areas indicate surface water bodies or soil taxonomic groups with no or limited *in-situ* lattice water sampling (see Table 2.1).

2.3.2 Comparison of In-situ and Remotely Sensed Vegetation Calibration Parameters

Using the 11 years of destructive vegetation sampling from 3 fields near Mead, NE, we found that the *GrWDRVI* was able to predict *SWB* when partitioning the data into maize and soybean, irrigated and rainfed, and green-up/mature and senescence periods of crop development (Figure 2.4 and Tables S2.2 and 2.3). Figure 2.4a and 2.4b illustrate the logistic functions that were used to predict *SWB* for maize green-up (RMSE = 0.88 kg/m^2) and soybean green-up

(RMSE = 0.47 kg/m^2). We note that *SWB* relationships with *GrWDRVI* indicate that *GrWDRVI* values less than 0.25 equated to the absence of *SWB*. During senescence, we found that a second order power law function fit the data well. We found the maize senescence functions (DOY> 210) needed to be further partitioned by irrigated and rainfed conditions as limitations in soil water will occur more quickly with mature plants that utilize the entire root zone. The resulting functions for irrigated maize during senescence (RMSE = 0.75 kg/m^2) and rainfed maize during senescence (RMSE = 0.92 kg/m^2) behaved well. For the soybean senescence function (DOY>230), we found a single function behaved reasonably well for both irrigated and rainfed conditions (RMSE = 0.45 kg/m^2). As expected from previous research (Ciganda et al, 2008; Peng et al. 2011), we found that the *GrWDRVI* was a poor predictor of *SDB*/percent water content of the vegetation. We will discuss these reasons and alternative strategies for estimating *SDB* in section 4.2.

		Green-up		Senescense	
		GrWDRI < 0.25	**GrWDRI >= 0.25**	**GrWDRI < 0.25**	**GrWDRI >= 0.25**
Maize	**Rainfed**	0	y=8/(1+exp(-9.844(x-0.501)))-0.618, RMSE = 0.88 kg/m^2	0	y=-1.354x^(-1.351)+8.817, RMSE = 0.75 kg/m^2
	Irrigated				y=-0.1348x^(-2.875)+7.256, RMSE = 0.92 kg/m^2
Soybean	**Rainfed**	0	y=4/(1+exp(-7.542(x-0.6085)))-0.247, RMSE = 0.47 kg/m^2	0	y=-0.1483x^(-2.225)+3.243, RMSE = 0.45 kg/m^2
	Irrigated				

Table 2.3: Summary of derived equations estimating standing wet biomass from *GrWDRVI* for maize and soybean partitioned into irrigated and rainfed areas and green-up (DOY< 210 for maize, DOY<230 for soybean) and senescence. Destructive biomass data is aggregated from 3 fields near Mead, NE between 2003-2013 (Table S2.2). We note that the maize and soybean functions were bounded to provide realistic behavior at the observed *GrWDRVI* and destructive vegetation sampling bounds. See main text for details.

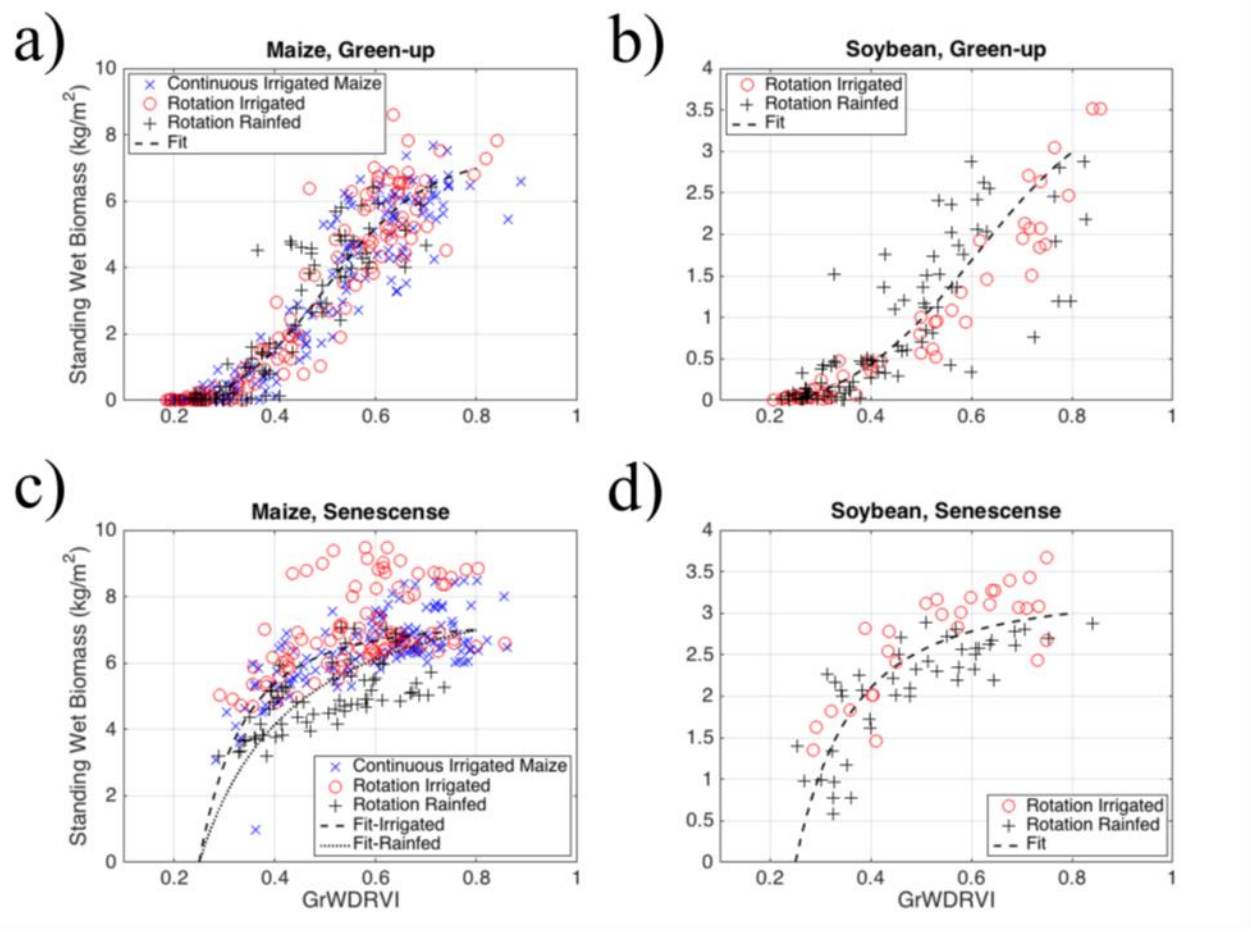

Figure 2.4: Relationship between *GrWDRVI* and observed standing weight biomass for maize (a, c) and soybean (b, d) partitioned into green-up (DOY< 210 for maize, DOY<230 for soybean) and senescence. Destructive vegetation data is aggregated from 3 fields near Mead, NE between 2003-2013 (Table S2.2). The regression coefficients and equations are summarized in Table 2.3. Note that the maize and soybean functions were subject to the constraints in order to provide realistic behavior at the observed *GrWDRVI* and destructive vegetation sampling bounds. See main text for details.

Using the derived relationships from the three study sites near Mead, NE, we applied the equations to our two study sites near Waco, NE (~ 88 km from Mead, NE, Figure 2.5 and Tables 2.4 and 2.5). Figure 2.5 illustrates the time series of *SWB* using the 8 day MODIS product and derived equations for both field sites. The figure also illustrates the observed destructive sampling for 4 different sampling bouts. With the limited data, we found the time series of *SWB*

calculated from the MODIS data followed the expected green-up and senescence *SWB* behavior for both the irrigated maize and soybean. The *GrWDRVI* derived *SWB* largely captured the maximum observed value for both the irrigated maize (6.58 kg/m^2 vs. 6.2 kg/m^2) and irrigated soybean (2.61 kg/m^2 vs.1.81 kg/m^2). The largest discrepancy was during the maize green-up period (DOY 183) where the observed value was 2.4 kg/m^2 and ~4.0 kg/m^2 calculated from the *GrWDRVI*. While the derived equations behaved well for this limited validation dataset, the equations should be tested at additional sites where other crop and soil types may influence the function coefficients. Overall, the equations and regression fits resulting in RMSE < 1 kg/m^2 are within the uncertainty of destructive biomass sampling in crops (Franz et al., 2013; 2015). By having general *SWB* relationships (for eastern Nebraska) through time using the 8 day MODIS data, this could allow for reasonable biomass corrections to N_0 with minimal effects (<0.01 cm^3/cm^3) on the overall estimation of *SWC*.

DOY (2014)	GrWDRVI, Irrigated-Maize	GrWDRVI- Irrigated Soybean	Calculated Standing Wet Biomass- Irrigated Maize (kg/m^2)	Calculated Standing Wet Biomass- Irrigated Soybean (kg/m^2)
153	0.23	0.23	0.00	0.00
161	0.24	0.24	0.00	0.00
169	0.32	0.28	0.53	0.06
177	0.57	0.54	4.69	1.25
185	0.55	NA	4.33	NA
193	0.63	0.63	5.63	1.91
201	0.61	0.71	5.34	2.48
209	0.55	0.73	6.50*	2.61
217	0.57	0.74	6.58	2.67
225	0.50	0.73	6.27	2.61
233	0.47	0.74	6.07	NA
241	0.40	0.68	5.38	2.89
249	0.43	0.64	5.73	6.77
257	0.27	0.47	1.44	6.07
265	0.25	0.44	0.00	5.83
281	0.21	0.28	0.00	2.02
289	0.21	0.26	0.00	0.78
297	0.20	0.25	0.00	0.00

Table 2.4: Summary of 2014 *GrWDRVI* and calculated standing wet biomass for irrigated maize and irrigated soybean fields near Waco, NE. Note that the senescence equation was applied to DOY 209 for the irrigated maize field as planting date and development can vary locally. The drop in *GrWDRVI* between DOY 201 and 209 is a clear indicator of change in plant growth stage that can be used on a field by field basis.

DOY (2014), Irrigated Soybean	Observed Standing Wet Biomass- Irrigated Soybean (kg/m^2)	DOY (2014), Irrigated Maize	Observed Standing Wet Biomass- Irrigated Maize (kg/m^2)
167	0.19	161	0.13
196	1.63	183	2.40
211	1.81	217	6.22
259	1.63	259	0.30

Table 2.5: Summary of 2014 observed standing wet biomass for irrigated maize and irrigated soybean fields near Waco, NE. The observations represent the aggregation of 18 plants collected at 6 different locations across the field on the sampling date.

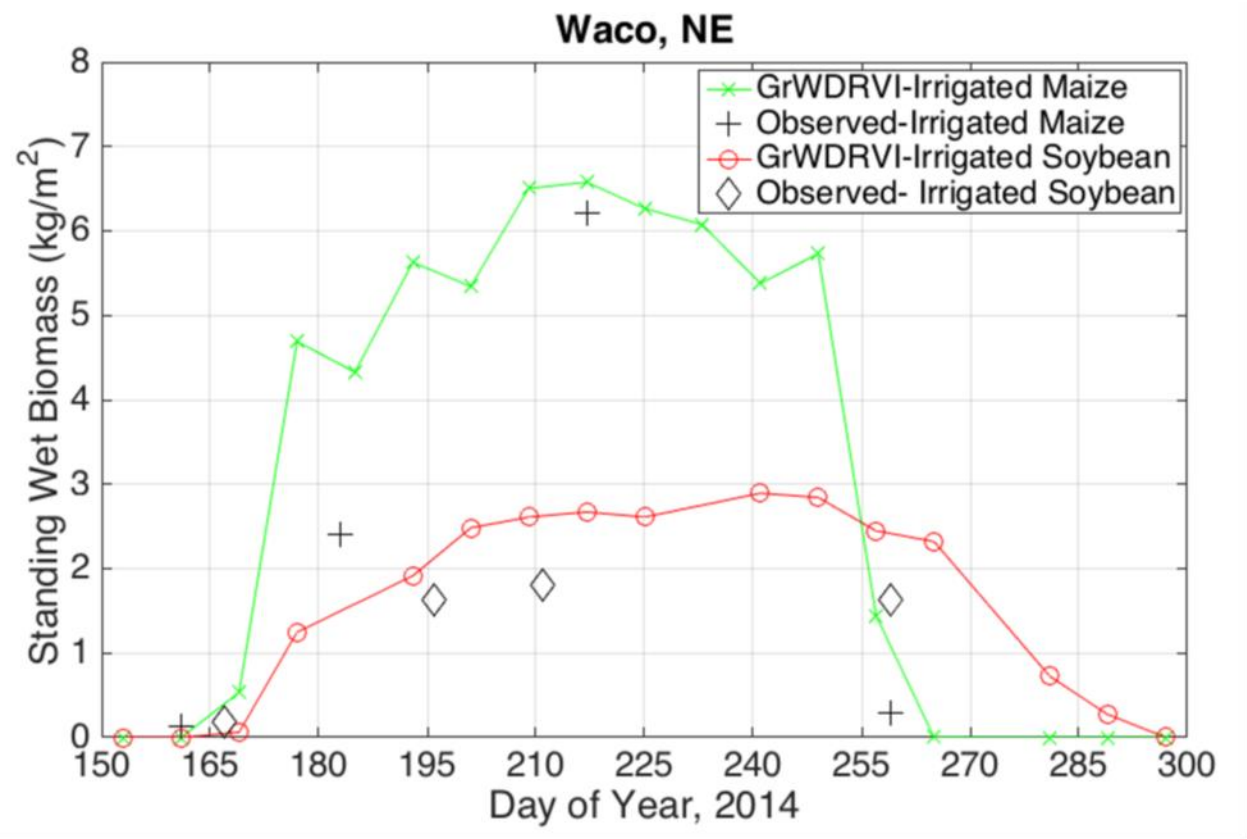

Figure 2.5: Time series of standing wet biomass for two study sites (irrigated maize and irrigated soybean) near Waco, NE over the 2014 growing season. The graph contains the observed *in-situ* sampling in addition to the *GrWDRVI* estimates using the equations summarized in Table 2.3. See Table 2.4 for *GrWDRVI* values and Table 2.5 for *in-situ* estimates.

2.3.3 Error Propagation Analysis of GSDE Soil Properties

In order to further assess the accuracy of our datasets, we synthetically altered the parameters via a Monte Carlo error analysis. This was done using the GSDE soil parameters (θ_{LW}, θ_{SOC}, and ρ_b) as compared to using local sampling (Figure 2.6). The analysis revealed that for the given bounds of θ_{LW}, θ_{SOC}, and ρ_b, the maximum RSME was around 0.035 cm^3/cm^3 at a *SWC* = 0.40 cm^3/cm^3. The asymmetric shape of all the curves is expected given the nonlinear calibration function given in Eq. (4) and the bounded nature of soil moisture. We found that ρ_b was by far the most sensitive parameter, followed by θ_{LW} and then θ_{SOC}. We expect the influence of vegetation changes to be small on the overall accuracy of *SWC* (<0.01 cm^3/cm^3) given the low RMSE described in section 3.2 (< 1 kg/m^2, which is ~1 mm of water or 0.0033 cm^3/cm^3 for a soil depth of 300 mm), We also note the critical factor in the error propagation analysis is the assumed range of ρ_b, given that it is directly multiplied by the gravimetric water content in the calibration function. *Therefore, future sampling efforts or evaluations of available datasets should seek to minimize the range of bulk density.*

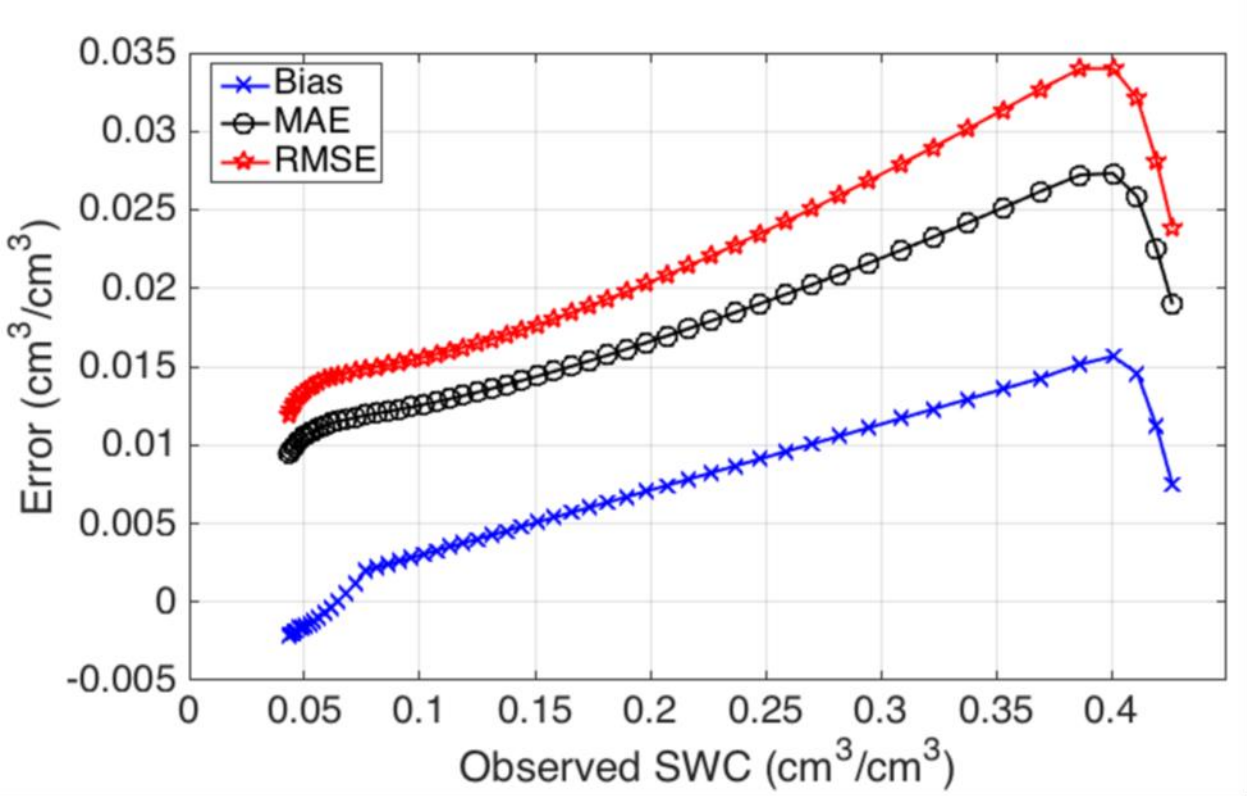

Figure 2.6: Propagation of error analysis using Monte Carlo simulations of 100,000 soil parameter datasets of true soil parameters (i.e. soil bulk density, lattice water, soil organic carbon) and perturbed parameters with matching mean differences and covariance matrix between *in-situ* samples and GSDE derived parameters (see Table 2.2). Three error metrics are presented across a range of neutron counts (and thus SWC values). Note that soil bulk density was constrained to 1.2-1.5 g/cm^3, lattice water was constrained from 1-8 wt. %, soil organic carbon was constrained from 0-8 wt. %, and soil water content was constrained from 0.03-0.45 cm^3/cm^3. Simulated and calculated values outside of these bounds were either reset to the minimum or maximum or removed from the Monte Carlo statistics. A minimum threshold of 70% of simulated cases were used to compute error statistics.

2.4 Discussion

2.4.1 Global Soil Calibration Parameters

The correlation between observed and GSDE clay content was very strong (Figure 2.2a) for all 61 sites in the CONUS except for the site in south central Texas. The site occurred near a transition from vertisol to alfisol soil taxonomic groups; the site may have been improperly

categorized (Table S2.1) or may have straddled a sharp gradient in clay contents. The strong correlation of the GSDE clay content with the observed values allowed us to use the GSDE clay content in understanding the correlation between clay content and lattice water organized by US soil taxonomic groups (Table 2.1). A strong correlation was only found for clay content and lattice water for the mollisol soil taxonomic group (see Greacen, 1981; Zreda et al., 2012). This strong correlation is significant because large portions of the Midwest and Great Plains regions of the United States are made up of mollisol soils. Globally, mollisol soils comprise about 7% of the land surface (United Nations 2007) but contain some of the highest productive grassland and crop areas (i.e. Central USA, Argentina, Central Eurasia). As such, the roving CRNP method remains applicable within grassland agricultural settings. No significant linear relationships with clay content were found for alfisol, aridisol, entisol, inceptisol, spodosol, or ultisol. Instead the mean value was assigned to the alfisol, aridisol, entisol, inceptisol, spodosol, and ultisol soil taxonomic groups when generating the CONUS map. We found the differences in most of the soil taxonomic mean values were statistically significant among different taxonomic groups given the small standard errors of the means (not shown but can be calculated from data in Table 2.1). The current analysis did not contain enough samples for the soil taxonomic groups of andisol, gelisol, histosol, oxisol, or vertisol to perform a linear regression or assign a mean value. We recommend future work to consider repeating the analysis for a larger dataset using the FAO 2007 (United Nations 2007) soil classification of all 25 groups (also classified for our sites in Table S2.1). Given the widespread interest in both the fixed and roving cosmic-ray technology, a database of lattice water and clay content for each site could be developed. In addition, warehouses like the Natural Resources Conservation Service (NRCS) in Lincoln, NE contain stored samples from around the USA. This warehouse with others around the globe could be

further sampled to help complete the global dataset for use by the cosmic-ray community. Finally, the NRCS regularly updates the Soil Survey Geographic Database (SSURGO), which contains higher spatial resolution and vertically resolved estimates of soil texture and structure (i.e. clay content and bulk density). With the defined regression relationships and soil taxonomic groups, better spatial maps of lattice water could be generated. This may become important for applications of the rover at scales less than 1 km, such as using it for applications in precision agriculture.

The correlation between the observed and GSDE soil organic carbon was fairly poor, particularly at the high end (> 4 wt. %). The history of land use is critical in determining carbon pools and how they change through time (Post et al., 2000) and may not be well represented in the GSDE. However, we note that organic carbon has a relatively small impact on the calibration function as it is multiplied by several factors in the calibration equation. For rover survey experiments, we suggest that this be sampled with composite samples, particularly between sites with varying land use histories which can be identified using historical land cover maps.

Observed *in-situ* soil bulk density and GSDE bulk density exhibited a positive relationship, albeit with low R^2. The poor fit and sensitivity of the parameter in the calibration function increases the importance of identifying the range and variability of bulk density within the rover sample domain. The variability shown here by the standard deviation of the bulk density for the individual point samples within the 28 ha sample domain varied between 0.1 and 0.2 g/cm^3. Moreover, minimizing the expected range of bulk density at a site is key given the propagation of error analysis presented in section 3.3. Thus, this result supports direct sampling at key locations (along gradients of land use, soil taxonomic groups, etc.) to constrain the range of expected bulk density values. We also suggest that for rover surveys in the USA (and

elsewhere), additional higher resolution datasets like SSURGO be used instead of the 1 km GSDE (in particular bulk density data as a function of depth), as significant small scale variability may be averaged out. This may be critical to account for in future roving CRNP research areas, such as precision agriculture or small scale watershed monitoring where significant soil texture variation may exist at short length scales.

2.4.2 Global Remotely Sensed Vegetation Calibration Parameters

The comparison of 11 years of destructive vegetation samples from maize and soybeans at 3 sites in eastern Nebraska indicated that the *GrWDRVI* was able to predict *SWB* in agricultural fields, especially when partitioned into green-up vs. senescence and irrigated vs. rainfed (Figure 2.4). However, as expected the *GrWDRVI* was unable to predict *SDB*. The main reason is as the plants begin to dry out during the late summer and early fall, leaves lose their chlorophyll and leaf structure beings to collapse thereby increasing reflected green and reducing near-infrared light (Ciganda et al. 2008; Peng et al. 2011). This is exaggerated by a change in the allocation of resources by the plant from leaves to grain, shifting where the majority of mass is located and thus weakening the capacity for the *GrWDRVI* to predict *SDB*. This biological investment of resources is more pronounced for maize than soybeans. As additional crops are included in this analysis, the location and development of the fruit and seed will impact the predictive relationships using vegetation indices.

While the developed regression relationships for maize and soybean (Table 2.3) were tested against independent biomass estimates from Waco, NE (Figure 2.5), we note that further validation is needed. In terms of a strategy for estimating *SDB*, we suggest that proxies such as

crop type and growth stage be used. Franz et al. (2013 and 2015) found that in early stages, maize and soybean had canopy water contents from 75-90 wt. %. By the end of senescence before harvest, the canopy water contents were down to 25-35 wt. %. If growth stage is not directly known, local meteorological observations, planting date, and crop variety can be used to compute proxies (e.g. growing degree days) or simulated from crop models (Allen et al. 1998). We note that having a reasonably accurate estimate of *SWB* and thus *BWE* (within ~ 1 kg/m^2) is all that is required to have a relatively small impact (< 0.01 cm^3/cm^3) on the estimated *SWC*. Finally, we note that this methodology is not applicable to areas with woody biomass. Following Franz et al., (2013), Hawdon et al., (2014), Baatz et al., (2015), and Coopersmith et al., (2014) we suggest other vegetation relationships (i.e. *BWE* vs. N_0) be defined. However, given the relatively small changes in *BWE* over the year in forests, we would expect small changes in N_0 through time.

2.5 Summary and Conclusions

In this chapter, we developed a framework using globally available datasets for estimating four (θ_{LW}, θ_{SOC}, ρ_b, SWB) of the five key soil and vegetation parameters needed by the cosmic-ray neutron method for estimating *SWC* in fast growing vegetation areas such as row crop production in agricultural areas. The remaining crop vegetation parameter (*SDB*) can be fairly well approximated by crop type, growth stage or simulated with crop models. The accuracy of the GSDE soil database was tested against 61 calibration datasets from the CONUS. We found that the 1 km GSDE compares well against observed clay content ($R^2 = 0.68$) but much poorer against soil bulk density ($R^2 = 0.203$) and soil organic carbon ($R^2 = 0.175$). Surprisingly, of the six soil taxonomic groups we investigated, only mollisols showed a

statistically significant correlation with clay content. The remaining five soil taxonomic groups we investigated did show statistically significant different mean values. These mean values were used to generate a map (not complete) of lattice water for the CONUS. From 11 years of destructive sampling of maize and soybean fields in eastern Nebraska, we found that the 8-day 500 m resolution MODIS derived *GrWDRVI* was highly correlated to *SWB*, particularly when partitioning the fields into green-up vs. senescence and irrigated vs. rainfed (RMSE < 1 kg/m^2). A propagation of error analysis indicated that the range of bulk density values was the most sensitive calibration parameter. For the selected ranges, we found the GSDE vs. local sampling resulted in a maximum RMSE of 0.035 cm^3/cm^3 at a *SWC* = 0.40 cm^3/cm^3.

With the continuing use of the roving CNRP we make the following recommendations on best calibration and use:

1) Collect a series (minimum of 7) of full calibration datasets ($\theta_{LW}, \theta_{SOC}, \rho_b, SWB, SDB$) in differing land use and soil types to estimate the instrument specific slope and intercept for correction factor N_0.
2) In the rover sampling area, construct a map of land use including: vegetation/crop type, planting date, variety, rainfed vs. irrigated, and gravel vs. paved roads vs. natural areas.
3) Collect a series of aggregate soil samples for soil organic carbon and lattice water around the survey area. The samples should be collected across land use, soil texture, and soil taxonomic groups. The GSDE or more local datasets like SSURGO in the USA can be used to select sites, cross validate samples, and fill in missing areas.
4) Soil bulk density is the critical parameter in the calibration equations and overall accuracy of the cosmic-ray neutron method. Bulk density should be collected locally

wherever possible. More local datasets like SSURGO in the USA will likely perform better at smaller scales than the 1 km GSDE.

5) *SWC* validation datasets should be collected to independently assess the accuracy of the rover survey results.

Chapter 3: Discussion on the Incorporation of Cosmic-ray Neutron Probe Soil Moisture Data into the Variable Infiltration Capacity Land Surface Model

3.1 Soil Moisture and Modeling

Effective water resource management is an important part of food security. This form of resource management requires an understanding of hydrologic processes on both a local and regional scale. This information is often generated via hydrologic models aimed at predicting cycles of water, energy, and nutrients. Hydrologic models and the knowledge they provide are likely to play a major role in future water management policy. Soil moisture, is a key component in agricultural development and water management decisions. It is equally important in the proper use of hydrologic models.

The hydrologic cycle is connected to the energy budget of the surface of the Earth by the innate capacity of soil moisture to regulate latent heat flux (Houser et al., 1998). Additionally, the presence of soil moisture in the root zone of vegetation plays a role in regulating precipitation patterns, streamflow generation, and evapotranspiration. Due to the significant coupling of soil moisture to global hydrologic fluxes, accurate simulation or observation of subsurface water has been shown to be valuable in hydrologic modeling (Wang, 2014; Brunner et al., 2012; Jung et al., 2010; Koster et al., 2004; Nijssen et al., 2001). Observations of soil moisture can be used in lieu of other parts of the water cycle (e.g. streamflow, evapotranspiration, storage, etc.) to validate the accuracy of models. However, model parameterization via soil moisture is difficult due to the high variability of soil moisture in space and time. Therefore, understanding the natural heterogeneity of soil moisture is a key challenge to predicting and describing

hydrogeophysical processes between the land and the atmosphere. Spatial variability in soil moisture causes difficulty in obtaining measurements over large areas or at significantly high resolutions. Because of this, many standard models are lacking proper soil water content (SWC) information in terms of spatial and temporal resolution (Vereecken et al., 2008). In addition, many models are moving towards higher spatial resolutions (~ 1 km, known as hyperresolution) while maintaining a regional or global scope (Wood et al., 2011). This approach may be supplemented via the use of other satellite soil moisture data such as NASA's SMAP and SMOS missions (Entekhabi et al., 2010; Kerr et al., 2010).

This trend has driven a need for networks designed to monitor SWC on intermediate and large spatial scales (Hinnell et al., 2010; Robinson et al., 2008a; Robinson et al., 2008b; Day-Lewis and Lane, 2004; and Binley and Beven, 2003). Many efforts have been made to characterize SWC over large spatial scales, consisting mainly of networks of in-situ point based sensors (e.g. Oklahoma Mesonet, Soil Climate Analysis Network (SCAN), Cosmic-ray Soil Moisture Observation System (COSMOS) etc.) arrayed across the world.

Unfortunately, these networks have somewhat limited spatial coherence due to the nature of point based sensing only representing the point at which they are placed. To date, our understanding of soil moisture information has been somewhat restricted to a scaling up of in-situ point based measurements (Famiglietti et al., 2008; Crow et al., 2012; Robinson et al., 2008). This approach to data generation can carry inherent uncertainties capable of limiting the accuracy of the model in which they are used.

Other SWC monitoring networks provide data at very large scales via the use of satellites [3, 9, and 36 km, NASA's Soil Moisture Active Passive (SMAP) and Europe's Soil Moisture and Ocean Salinity (SMOS) Satellites]. However, these approaches often cannot represent water

content deeper than ~ 2 cm and may often fail to capture the active root zone of the soil column (Jackson et al., 1997; Crow et al., 2012). The contrast between point based sensors and satellite imagery continues to cause debate amongst hydrologists and water balance modelers.

To develop SWC monitoring networks that possess the advantages of detailed point based measurements and large scale satellite systems, novel geophysical techniques are required (Zreda et al., 2012; Franz et al., 2012; Binley et al. 2015; Franz et al., 2015). Geophysical strategies that are capable of merging point and remotely sensed data into a cohesive structure have the potential to minimize the disadvantages of networks currently in place. Recent years have seen the emergence of the Cosmic-ray Neutron Probe (CRNP) as a viable technique for SWC monitoring and data merging over varying spatial scales (Zreda et al., 2012; Franz et al., 2012; Binley et al. 2015). This hydrogeophysical method has been demonstrated to be functional on a small and large spatial scale within both agricultural and natural environments (Franz et al., 2012; Zreda et al., 2012; Franz et al., 2015).

This chapter seeks to address the advantages of the CRNP technique as a tool for the monitoring of SWC over differing spatial scales. Specifically, the suitability of the CRNP for use as a SWC data generation tool within hydrological modeling will be discussed. This concept will be presented within the framework of the Variable Infiltration Capacity Model (VIC) in terms of instrument resolution and data heterogeneity. Most importantly, the applicability of the CRNP technology for water management in the coming decades will be explored.

3.2 The Variable Infiltration Capacity Model

The VIC model is a commonly used hydrologic model first described by Wood et al. (1992) and Liang et al., (1994). This model assumes that the capacity for precipitation infiltration into the soil column is a highly variable parameter due primarily to spatial changes in topography, soil type, and vegetation structure (Wood et al., 1992). The VIC model attributes runoff generation and evapotranspiration to these parameters as well as their variability in space across a landscape or catchment. Modeling water and weather cycles on a global scale via general circulation models (GCMs) often requires accurate representations of land-atmosphere interactions. LSMs such as VIC are often connected to GCMs as a tool for effectively incorporating surface and sub-surface hydrological processes in weather and climate prediction (Liang et al., 1994; Liang et al., 1996; Manabe, 1969; Manabe et al., 1965).

Parameterization of vegetation and infiltration is easier said than done due primarily to the large scale of GCMs and the difficulty of estimating land surface interactions such a scale (Wood et al., 1992). This difficulty is typically mitigated via the use of remote sensing to generate observations for GCMs. This has become more common as water science has progressed (Wood et al., 2011).

The VIC model was originally designed to represent an area within a catchment as a single soil layer (Stamm et al., 1994). Stamm et al., (1994), proposed that this approach is not adequate for LSMs or their subsequent incorporation into global models. The single layer VIC approach was concluded to be inferior to a two layer approach (VIC-2L) that is better capable of characterizing surface evaporation and by extension the water cycle (Stamm et al., 1994). The development of a two layer VIC model was conducted by Liang et al., (1994) and Liang et al., (1996). Current versions of VIC have 3 soil layers and a canopy layer with up to 11 vegetation types plus bare soil. When tested in-situ, the VIC-2L model was able to accurately represent land surface

interactions and hydrologic flow. This innovative approach to the VIC model was intended to take into account the heterogeneity of precipitation infiltration as well as variable vegetation characteristics (Liang et al., 1994, 1996). Additionally, water drainage from upper layers of the soil to deeper layers, thus generating subsurface flow of groundwater was also considered (Liang et al., 1994; 1996).

3.3 Modeling Applications of the Cosmic-ray Neutron Probe

Like all hydrologic models, VIC requires accurate soil moisture data for its proper functioning. Unfortunately, accumulating SWC data on the larger scales necessary for incorporation of VIC into GCMs is impractical with standard point based in-situ measurements. Large scale monitoring is possible via satellite techniques yet often lacks the appropriate resolution in both space and time as well as penetration depth. The high spatiotemporal resolution of the CRNP as well as its capacity for large and small scale applications, provides a distinct advantage to other SWC monitoring strategies.

The penetration "sight" of the CRNP (~30 cm) captures a greater extent of the active root zone responsible for much of the streamflow and hydrologic activity modeled within VIC. This lends increased predictive power to the SWC data generated via the CRNP. Understanding the SWC dynamics in the active root zone may provide the ability to more accurately model the hydrology of deeper soil layers in that, the more information available about the near surface the more confident predictions can be about deep percolation, infiltration, and sub-surface flow.

Many hydrologic models rely on simulated or observational data organized in a grid cell manner. However, natural catchments are not regular shapes. The CRNP in both its mobile and stationary form has the capacity to generate SWC information fitting the irregular area of any

particular natural watershed. This minimizes any error associated with other forms of mapping such as satellite remote sensing and allows for models to predict water cycle behavior with greater accuracy.

Once the calibration process has been performed (see sec. 1.2), the SWC information generated by the CRNP can be used to verify if a model is functioning correctly (model validation), provide the initial conditions of the model, or both. These observational data can be incorporated from the first simulated day of a model until the end rather than relying solely on simulated SWC data.

3.4 Summary and Conclusions

This chapter discusses the advantages of the Cosmic-ray Neutron Probe for use as a soil water content observational tool. Additionally, this use is examined from the context of incorporation as a validation and parameterization method within hydrologic models, in particular the Variable Infiltration Capacity model. The importance of soil moisture in the global hydrologic cycle is investigated, as well as its importance in modeling as a validation tool. The advantages and disadvantages of traditional SWC monitoring networks are compared to the CRNP. Specifically, the lack of appropriate resolution and penetration depth of satellites and the limited scale and area representation of point based measurement systems. There is a need for accurate SWC data that can compete with the ever increasing resolution and scale of global circulation and land surface models. Both effective water resource management and production agriculture is often performed with the use of water balance models. This trend is likely to continue in the coming decades only increasing the need for SWC data that can be accessed in a versatile manner and at the scales and resolutions necessary. The CRNP is a likely candidate to

fill this role. As an emerging technology this method has great potential for use in a variety of situations from water balance modeling to agriculture and beyond.

Chapter 4: Conclusions

This thesis explores the use of the Cosmic-ray Neutron Probe as a tool for the monitoring and detection of soil water. Specifically, its use as a mobile roving device capable of collecting soil water information over large spatial areas is shown. Large globally available datasets are shown to be capable of incorporation into the calibration process of this technology with sufficiently small error. This is shown to be a viable technique for accurate data generation via the mobile Cosmic-ray Neutron Probe. The potential of this technology for incorporation into production agriculture and as a source of data for hydrologic modeling (specifically the Variable Infiltration Capacity model) is discussed. The future of precision agriculture and water resource management is intrinsically tied to the future of global food security. The Cosmic-ray Neutron Probe may play a part in addressing that challenge, so that ultimately more food can be produced with less impact on groundwater.

References

Allen, R. G., L. S. Pereira, D. Raes, and M. Smith, Crop evapotranspiration. Guidelines for Computing Crop Water Requirements. FAO Irrigation and Drainage Paper 56., Food and Agriculture Organization of the United Nations, Rome, Italy. 1998.

Baatz R., Bogena H. R., Hendricks Franssen H. J., Huisman J. A., and Montzka C. An Empirical Vegetation Correction for Soil Water Content Quantification Using Cosmic Ray Probes, *Water Resources Research*, Vol. 51, No.4, Pgs. 2030-2046, 2015.

Beven K. J., and Cloke H. L. Comment on "Hyperresolution global land surface modeling: Meeting a grand challenge for monitoring Earth's terrestrial water" by Eric F. Wood et al., *Water Resour. Res.*, Vol. 48, W01801, doi:10.1029/2011WR010982, 2012.

Binley A., Hubbard S. S., Huisman J. A., Revil A., Robinson D. A., Singha K., and Slater L. D.: The Emergence of Hydrogeophysics for Improved Understanding of Subsurface Processes Over Multiple Time Scales, *Water Resour. Res.*, Vol. 51, doi:10.1002/2015WR017016, 2015.

Binley, A., and K. Beven. Vadose zone flow model uncertainty as conditioned on geophysical data. *Ground Water*. Vol. 41, No. 2, Pgs. 119–127. doi:10.1111/j.1745-6584.2003.tb02576.x, 2003.

Bogena H. R., Huisman J. A., Baatz R., Hendricks Frassen H. J., and Vereecken H.: Accuracy of the Cosmic-Ray Soil Water Content Probe in Humid Forest Ecosystems: The Worst Case Scenario, *Water Resour. Res.*, Vol. 49, Pgs. 5778-5791, doi:10.1002/wrcr.20463, 2013.

Brunner P., Doherty J., and Simmons C. T. Uncertainty assessment and implications for data acquisition in support of integrated hydrologic models, *Water Resour.* Res., Vol. 48, doi:10.1029/2011WR011342, 2012.

Chrisman B. B. and M. Zreda: Quantifying Mesoscale Soil Moisture with the Cosmic-Ray Rover, *Hydrology and Earth System Sciences*, Vol. 17, No. 12, Pgs. 5097 – 5108, 2013.

Ciganda, V., Gitelson, A.A., and Schepers, J. Vertical Profile and Temporal Variation of Chlorophyll in Maize Canopy: Quantitative "Crop Vigor" Indicator by Means of Reflectance-Based Techniques, *Agronomy Journal*, Vol. 100, No. 5, Pgs. 1409-1417, doi:10.2134/agronj2007.0322, 2008.

Coopersmith E. J., Cosh M. H., and Daughtry C. S. T.: Field-Scale Moisture Estimates using COSMOS Sensors: A Validation Study with Temporary Networks and Leaf-Area Indices, *Journal of Hydrology*, Vol. 519, Part A, Pgs. 637-643, http://dx.doi.org/10.1016/j.jhydrol.20 14.07.060, 2014.

Crow, W. T., A. A. Berg, M. H. Cosh, A. Loew, B. P. Mohanty, R. Panciera, P. de Rosnay, D. Ryu, and J. P. Walker: Upscaling Sparse Ground-Based Soil Moisture Observations For The Validation Of Coarse-Resolution Satellite Soil Moisture Products. *Rev. Geophys*. 50. doi:10.1029/2011rg000372, 2012.

Dane, J. H., and C. G. Topp. Methods of Soil Analysis: Part 4 Physical Methods. Soil Science Society of America. Madison, WI. 2002.

Day-Lewis, F. D., and J. W. Lane. Assessing the resolution-dependent utility of tomograms for geostatistics. *Geophysical Research Letters*. Vol. 31, No. 7, doi:10.1029/2004gl019617, 2004.

Desilets D., and Zreda M.: Footprint Diameter for a Cosmic-Ray Soil Moisture Probe: Theory and Monte Carlo Simulations, *Water Resour. Res*., Vol. 49, Pgs. 3566–3575, doi:10.1002/wrcr.20187, 2013.

Desilets D., Zreda M., Ferre T. P. A.: Nature's Neutron Probe: Land Surface Hydrology at an Elusive Scale with Cosmic-Rays, *Water Resour. Res*., Vol. 56, doi:10.1029/2009wr008726, 2010.

Dong J. N., Ochsner T. E., Zreda M., Cosh M. H., and Zou C. B.: Calibration and Validation of the COSMOS Rover for Surface Soil Moisture Measurement, *Vadose Zone J.*, Vol. 13, No. 4, doi:10.2136/vzj2013.08.0148, 2014.

Entekhabi D., Njoku E. G., Neill P. E., Kellogg K. H., Crow W. T., Edelstein W. N., and Kimball J.: The Soil Moisture Active Passive (SMAP) Mission, *Proceedings of the IEEE*, Vol. 98, No. 5, Pgs. 704-716, 2010.

Famiglietti, J. S., D. Ryu, A. A. Berg, M. Rodell, and T. J. Jackson. Field observations of soil moisture variability across scales, *Water Resour. Res*., Vol. 44, doi:10.1029/2006WR005804, 2008.

Franz T. E., Wang T., Avery W., Finkenbiner C., and Brocca L.: Combined Analysis of Soil Moisture Measurements from Roving and Fixed Cosmic-Ray Neutron Probes for Multiscale Real-Time Monitoring, *Geophys. Res. Lett*., Vol. 42, doi:10.1002/ 2015GL063963, 2015.

Franz T. E., Zreda M., Ferre P. A., Rosolem R., Zweck C., Stillman S., Zeng X., and Shutt W. J.: Measurement Depth of The Cosmic-Ray Soil Moisture Probe Affected by Hydrogen From Various Sources. *Water Resour. Res.*, Vol. 48, (in press), doi: 10.1029/2012WR011871, 2012.

Franz T. E., Zreda M., Rosolem R., Hornbuckle B. K., Irvin S. L., Adams H., Kolb T. E., Zweck C., and Shuttleworth W. J.; Ecosystem-Scale Measurements of Biomass Water using Cosmic-ray Neutrons, *Geophysical Research Letters*, Vol. 40, Pgs. 1–5, doi:10.1002/grl.50791, 2013.

Gietelson, A.A., Wide Dynamic Range Vegetation Index for Remote Quantification of Biophysical Characteristics of Vegetation, Journal of Plant Physiology, Vol. 161, Pgs. 165-173, 2004.

Greacen, E.L.: Soil water assessment by the neutron method, Australia: CSIRO. 1981.

Hawdon A., McJannet D., and Wallace J.: Calibration and Correction Procedures for Cosmic-Ray Neutron Soil Moisture Probes Located Across Australia, *Water Resour. Res.*, Vol. 50, Pgs. 5029–5043, doi:10.1002/2013WR015138, 2014.

Hinnell, A.C., T.P.A. Ferré, J.A. Vrugt, J.A. Huisman, S. Moysey, J. Rings, and M.B. Kowalsky. Improved Extraction of Hydrologic Information from Geophysical Data through Coupled Hydrogeophysical Inversion. *Water Resources Research*. Vol. 46, doi:10.1029/2008WR007060, 2010.

Houser P. R., Shuttleworth W. J., Famiglietti J. S., Gupta H. V., Syed K. H., and Goodrich D. C. Integration of Soil Moisture Remote Sensing and Hydrologic Modeling Using Data Assimilation, *Water Resour. Res.*, Vol. 34, No. 12, Pgs. 3405–3420, doi:10.1029/1998WR900001, 1998.

Iwema J., Rosolem R., Baatz R., Wagener T., and Bogena H. R.: Investigating Temporal Field Sampling Strategies for Site-Specific Calibration Of Three Soil Moisture-Neutron Intensity Parameterization Methods, *Hydrol. Earth Syst. Sci. Discuss.,* Vol. 12, Pgs. 2349-2389. doi:10.5194/hessd-12-2349-2015\, 2015.

Jackson, T.J., P.E. Oneill, and C.T. Swift. Passive microwave observation of diurnal surface soil moisture. IEEE *Trans. Geosci. Rem. Sens*. Vol. 35, No. 5, Pgs. 1210– 1222. doi:10.1109/36.628788, 1997.

Jung M., Reichstein M., Ciais P., Seneviratne S.I., Sheffield J., Goulden M.L., Bonan G., Cescatti A., Chen J., de Jeu R., A. Johanne, Dolman J., Eugster W., Gerten D., Gianelle D., Gobron N., Heinke J., Kimball J., Law B.E., Montagnani L., Mu Q., Mueller B., Oleson K., Papale D., Richardson A.D., Roupsard O., Running S., Tomelleri E., Viovy N., Weber U., Williams C., Wood E., Zaehle S. & Zhang K. Recent Decline In The Global Land Evapotranspiration Trend Due To Limited Moisture Supply. *Nature* Vol. 467, Pgs. 951–954. doi:10.1038/nature09396, 2010.

Kerr Y. H., Waldteufel P., Wigneron J. P., Delwart S., Cabot F. O., Boutin J., and Juglea S. E.: The SMOS Mission: New Tool for Monitoring Key Elements of the Global Water Cycle, *Proceedings of the IEEE*, Vol. 98, No. 5, Pgs. 666-687, 2010.

Köhli M., Schrön M., Zreda M., Schmidt U., Dietrich P., and Zacharias S.: Footprint Characteristics Revised for Field-Scale Soil Moisture Monitoring with Cosmic-Ray Neutrons, Water *Resources Research*. doi: 10.1002/2015WR017169, 2015.

Koster R.D., Dirmeyer P.A., Guo Z., Bonan G., Chan E., Cox P., Gordon C.T., Kanae S., Kowalczyk E., Lawrence D., Liu P., Lu C.H., Malyshev S., McAvaney B., Mitchell K., Mocko D., Oki T.,

Oleson K., Pitman A., Sud Y.C., Taylor C.M., Verseghy D., Vasic R., Xue Y., and Yamada T., Regions of Strong Coupling Between Soil Moisture and Precipitation. *Science*. Vol. 305, No. 5687, Pgs. 1138-1140, DOI:10.1126/science.1100217, 2004.

Liang X., Wood E.F., Lettenmaier D.P. Surface Soil Moisture Parameterization of the VIC-2L model: Evaluation and Modification. *Global and Planetary Change*. Vol. 13, Pgs. 195 – 206, 1996.

Liang X., Lettenmaier D.P, Wood E.F., Burges S.J. A Simple Hydrologically Based Model of Land Surface Water and Energy Fluxes for General Circulation Models. *Journal of Geophysical Research*, Vol. 99, No. D7, Pgs. 14,415 – 14,428, 1994.

Lv L., Franz T. E., Robinson D. A., and Jones S. B.: Measured and Modeled Soil Moisture Compared with Cosmic-Ray Neutron Probe Estimates in a Mixed Forest, *Vadose Zone Journal*, Vol. 13, No. 12, 2014.

Manabe S. Climate and the Ocean Circulation: The Atmospheric Circulation and the Hydrology of the Earth's Surface. *Monthly Weather Review*. Vol. 97, No. 11, 1969.

Manabe S., Smagorinsky J., Strickler R.F. Simulated Climatology of a General Circulation Model with a Hydrologic Cycle. *Monthly Weather Review*. Vol. 93, No. 12, 1965.

McJannet D., Franz T. E., Hawdon A., Boadle D., Baker B., Almeida A., Silberstein R., Lambert T., and Desilets D.: Field Testing of the Universal Calibration Function for Determination of Soil Moisture With Cosmic-Ray Neutrons, *Water Resour. Res.*, Vol. 50, Pgs. 5235–5248, doi:10.1002/2014WR015513, 2014.

Mekonnen M. M. and Hoekstra A. Y.: The Green, Blue and Grey Water Footprint of Crops and Derived Crop Products, *Hydrol. Earth Syst. Sci.*, Vol. 15, Pgs. 1577-1600, doi:10.5194/hess-15-1577-2011, 2011.

Nguy-Robertson A., Gitelson A., Peng Y., Viña A., Arkebauer T., and Rundquist D.: Green Leaf Area Index Estimation in Maize and Soybean: Combining Vegetation Indices to Achieve Maximal Sensitivity, *Agronomy Journal*, Vol. 104, No. 5, doi:10.2134/agronj2012.0065, 2012.

Nguy-Robertson, A.L., and Gitelson, A.A.: Algorithms for estimating green leaf area index in C3 and C4 crops for MODIS, Landsat TM/ETM+, MERIS, Sentinel MSI/OLCI, and Venus sensors, *Remote Sensing Letters*, Vol. 6, No. 5, doi: 10.1080/2150704X.2015.1034888, 2015.

Nijssen B., O'Donnell G.M., Hamlet A.F., and Lettenmaier D.P., Hydrologic Sensitivity of Global Rivers to Climate Change. *Climatic Change*. Vol. 50, No. 1, Pgs. 143-175, 2001.

Njoku E. G., and Entekhabi, D.: Passive Microwave Remote Sensing of Soil Moisture, *Journal of Hydrology*, Vol. 184, No. 1, Pgs. 101-129, 1996.

Peng, Y., Gitelson, A.A., Keydan, G., Rundquist, D.C., and Moses, W. Remote Estimation of Gross Primary Production in Maize and Support for a New Paradigm Based on Total Crop Chlorophyll Content, *Remote Sensing of Envirionment*, Vol. 115, Pgs. 978-989, doi:10.1016/j.rse.2010.12.001, 2011.

Post W. M., and Kwon K. C.: Soil Carbon Sequestration and Land-Use Change: Processes and Potential, *Global Change Biology*, Vol. 6, Pgs. 317-327, doi:10.1046/j.1365-2486.2000.00308.x, 2000.

Renzullo L. J., van Dijk A. I. J. M., Perraud J. M., Collins D., Henderson B., Jin H., Smith A. B., and McJannet D. L.: Continental Satellite Soil Moisture Data Assimilation Improves Root-Zone Moisture Analysis for Water Resources Assessment, *Journal of Hydrology*, Vol. 519, Part D, Pgs. 2747-2762, 2014.

Robinson D. A., Binley A., Crook N., Day-Lewis F. D., Ferre T. P. A., Grauch V. J. S., Knight R., Knoll M., Lakshmi V., Miller R., Nyquist J., Pellerin L., Singha K., and Slater L.: Advancing Process-Based Watershed Hydrological Research using Near-Surface Geophysics: A Vision for, and Review of, Electrical and Magnetic Geophysical Methods, *Hydrol. Processes*, Vol. 22, No. 18, Pgs. 3604-3635, 2008a

Robinson, D.A., C.S. Campbell, J.W. Hopmans, B.K. Hornbuckle, S.B. Jones, R. Knight, F. Ogden, J. Selker, and O. Wendroth. Soil moisture measurement for ecological and hydrological watershed-scale observatories: A review. *Vadose Zone J*. Vol. 7, No. 1, Pgs. 358–389. doi:10.2136/vzj2007.0143, 2008b.

Rosolem, R., W. J. Shuttleworth, M. Zreda, T. E. Franz, X. Zeng, and S. A. Kurc. The Effect of Atmospheric Water Vapor on the Cosmic-ray Soil Moisture Signal. J. Hydrometeorol. doi:10.1175/JHM-D-12-0120.1. 2013.

Rosolem R., Hoar T., Arellano A., Anderson J. L., Shuttleworth W. J., Zeng X., and Franz T. E.: Translating Aboveground Cosmic-Ray Neutron Intensity to High-Frequency Soil Moisture Profiles at Sub-Kilometer Scale, *Hydrol. Earth Syst. Sci*., Vol. 18, Pgs. 4363-4379, doi:10.5194/hess-18-4363-2014, 2014.

Shangguan W., Dai Y., Duan Q., Liu B., and Yuan H.: A global Soil Dataset for Earth System Modeling, *J. Adv. Model Earth Syst*., Vol. 6, Pgs. 249-263, doi:10.1002/2013MS000293, 2014.

Shuttleworth J., Rosolem R., Zreda M., and Franz T. E.: The Cosmic-Ray Soil Moisture Interaction Code (COSMIC) for use in Data Assimilation, *Hydrol. Earth Syst. Sci.*, Vol. 17, Pgs. 3205-3217, doi:10.5194/hess-17-3205-2013, 2013.

Stamm J.F., Wood E.F., Lettenmaier D.P. Sensitivity of a GCM Simulation of Global Climate to the Representation of Land-Surface Hydrology. *Journal of Climate*. Vol. 7, Pgs. 1218 – 1239, 1994.

Suyker A. E., Verma S. B., Burba G. G., and Arkebauer T. J.: Gross Primary Production and Ecosystem Respiration of Irrigated Maize and Irrigated Soybean During a Growing Season, *Agricultural Forest Meteorology*, Vol. 131, PGs. 180-190, 2005.

United Nations Department of Economic and Social Affairs (United Nations). World Population Prospects: The 2015 Revision.

United Nations Food and Agriculture Organization (FAO). How to Feed the World in 2050, High *Level Expert Forum*, Rome, Italy, 2009.

United Nations Food and Agriculture Organization (United Nations). IUSS Working Group WRB, World Reference Base for Soil Resources 2006, first update 2007. World Soil Resources Reports No. 103. FAO, Rome.

Vachaud G., Silans A. P. D. E., Balabanis P., Vauclin M.: Temporal Stability of Spatially Measured Soil Water Probability Density Function, *Soil Science Society of America Journal*, Vol. 49, Pgs. 822-828, 1985.

Vereecken H., Huisman J. A., Bogena H., Vanderborght J., Vrugt J. A., and Hopmans J. W.: On the Value of Soil Moisture Measurements in Vadose Zone Hydrology: A Review, *Water Resources Research*, Vol. 44, doi:10.1029/2008wr006829, 2008.

Viña A., Gitelson A. A., Nguy-Robertson A. L., and Peng Y.: Comparison of Different Vegetation Indices for the Remote Assessment of Green Leaf Area Index of Crops, *Remote Sensing of Environment*, Vol. 115, No. 12, Pgs. 3468-3478, 2011.

Wang T., Modeling The Impacts Of Soil Hydraulic Properties On Temporal Stability Of Soil Moisture Under A Semi-Arid Climate, *Journal of Hydrology*, Vol. 519, Part A, No. 27, Pgs. 1214-1224, http://dx.doi.org/10.1016/j.jhydrol.2014.08.052, 2014.

Wood E. F., Roundy J. K., Troy T. J., van Beek L. P. H., Bierkens M. F. P., Blyth E., de Roo A., Döll P., Ek M., Famiglietti J., Gochis D., van de Giesen N., Houser P., Jaffé P. R., Kollet S., Lehner B., Lettenmaier D. P., Peters-Lidard C., Murugesu S., Sheffield J., Wade A., and Whitehead P.: Hyperresolution Global Land Surface Modeling: Meeting a Grand Challenge for Monitoring Earth's Terrestrial Water, *Water Resources Research*., Vol. 47, doi:10.1029/2010WR010090, 2011.

Wood E.F., Lettenmaier D.P., and Zartarian V.G. A Land-Surface Hydrology Parameterization with Subgrid Variability for General Circulation Models. *Journal of Geophysical Research*. Vol. 97, No. D3 pgs. 2717 – 2728, 1992.

Zreda M., Desilets D., Ferre T. P. A., and Scott R. L.: Measuring Soil Moisture Content Non-Invasively at Intermediate Spatial Scale Using Cosmic-Ray Neutrons, *Geophys. Res. Lett.*, Vol. 35, No. 21, doi:10.1029/2008gl035655, 2008.

Zreda M., Shuttleworth W. J., Xeng X., Zweck C., Desilets D., Franz T. E., Rosolem R., and Ferre P. A.: COSMOS: The Cosmic-Ray Soil Moisture Observing System. *Hydrol. Earth Syst. Sci. Discuss*., Vol. 9, Pgs. 5405-4551, doi:10.5194/ hessd-9-4505-2012, 2012.

Appendix

					Onsite In-Situ Sampling (0-30 cm)								GSDE Product (average 0-30 cm)			
ID	Latitude	Longitude	USA Soil Classification (12 Classes)	Soil Classification from FAO 2007 (25 Classes)	Clay (Wt. %)	St. Dev. Clay (Wt. %)	Number Clay Wt. % Samples	Avg. Lattice Water (Wt. %)	St. Dev. Lattice Water (Wt. %)	Number of Lattice Water Samples	Organic Carbon (Wt. %)	Avg. Bulk Density (g/cm^3)	St. Dev. Bulk Density (g/cm^3)	Clay (Wt. %)	Avg. Lattice Water (Wt. %)	Organic Carbon (Wt. %)	Avg. Bulk Density (g/cm^3)
1	39.1006	-105.1025	Alfisol	Luvisols	NA	NA	NA	2.80	0.87	3	0.45	1.40	0.220	22.3	4.31	1.66	1.36
2	39.3232	-86.4131	Alfisol	Luvisols	24.03	6.28	15	3.25	0.40	4	1.21	1.38	0.120	18.3	4.31	1.37	1.40
3	38.4316	-120.9659	Alfisol	Luvisols	32.47	5.96	15	6.05	1.35	4	0.55	1.49	0.130	21.0	4.31	1.31	1.40
4	37.0310	-119.2564	Alfisol	Luvisols	16.41	5.55	15	4.78	0.77	4	3.25	1.02	0.190	19.3	4.31	1.20	1.44
5	37.0678	-119.1944	Alfisol	Luvisols	6.14	1.04	9	4.48	0.43	4	2.36	1.05	0.240	16.7	4.31	0.67	1.40
6	45.8205	-121.9519	Alfisol	Luvisols	11.00	3.50	15	6.28	1.02	4	3.80	0.89	0.090	10.7	4.31	1.57	1.00
7	46.9514	-110.8871	Alfisol	Luvisols	19.68	3.60	3	4.00	NA	1	1.11	NA	NA	15.0	4.31	1.15	1.43
8	41.3644	-106.2394	Alfisol	Luvisols	10.86	4.83	4	4.83	1.07	4	4.95	NA	NA	13.0	4.31	1.11	1.40
9	35.7397	-90.7620	Alfisol	Luvisols	23.27	2.87	3	2.33	0.68	1	1.33	NA	NA	15.3	4.31	0.86	1.50
10	31.5615	-110.1404	Aridisol	Yermosols	NA	NA	NA	4.00	NA	1	0.48	1.40	0.090	14.7	2.73	0.89	1.58
11	31.7438	-110.0219	Aridisol	Yermosols	NA	NA	NA	3.17	0.50	3	0.42	1.40	0.110	14.3	2.73	0.40	1.53
12	31.7368	-109.9418	Aridisol	Yermosols	NA	NA	NA	4.48	1.72	3	0.82	1.23	0.110	14.3	2.73	0.40	1.53
13	31.9085	-110.8394	Aridisol	Yermosols	NA	NA	NA	2.50	0.46	3	0.29	1.46	0.100	9.0	2.73	0.70	1.54
14	33.6094	-116.4506	Aridisol	Yermosols	13.15	7.36	15	1.79	0.30	13	0.17	1.58	0.110	16.7	2.73	0.25	1.49
15	34.5798	-111.8627	Aridisol	Yermosols	NA	NA	NA	2.40	NA	1	0.60	1.36	0.210	12.0	2.73	0.95	1.40
16	34.5766	-111.8585	Aridisol	Yermosols	NA	NA	NA	1.85	NA	1	0.55	1.50	0.200	12.0	2.73	0.95	1.40
17	44.4523	-121.5574	Aridisol	Xerosols	8.95	0.96	15	4.83	0.71	4	1.36	1.04	0.140	13.0	2.73	2.53	0.92
18	34.3999	-106.6743	Aridisol	Yermosols	NA	NA	NA	0.73	0.41	4	1.03	NA	NA	19.3	2.73	0.81	1.47
19	31.7442	-110.0518	Aridisol	Yermosols	NA	NA	NA	1.50	NA	1	3.65	NA	NA	14.3	2.73	0.40	1.53
20	31.2364	-84.4617	Entisol	Regosols	7.23	4.03	5	1.08	0.43	4	0.66	1.38	0.180	9.3	1.51	0.73	1.52
21	33.3828	-81.5660	Entisol	Regosols	6.61	2.17	5	0.88	0.49	4	0.53	1.41	0.260	12.0	1.51	0.98	1.57
22	42.0796	-101.4540	Entisol	Regosols	NA	NA	NA	3.00	NA	1	6.12	0.97	0.250	5.0	1.51	1.23	1.73
23	42.0722	-101.4411	Entisol	Regosols	NA	NA	NA	0.70	NA	1	0.46	1.46	0.130	5.0	1.51	1.23	1.73
24	42.0595	-101.4413	Entisol	Regosols	NA	NA	NA	1.70	NA	1	1.96	NA	NA	5.0	1.51	1.23	1.73
25	36.0635	-97.2170	Inceptisol	Cambisols	29.73	12.95	12	5.17	1.44	3	0.65	1.46	0.090	16.7	4.98	7.00	1.39
26	40.6646	-77.9067	Inceptisol	Cambisols	22.14	3.68	3	4.78	0.38	4	1.26	1.49	0.210	17.3	4.98	1.67	1.39
27	41.0121	-102.1038	Mollisol	Kastanozems	NA	NA	NA	1.70	NA	1	0.72	1.68	0.250	14.3	2.10	1.37	1.41
28	36.6054	-97.4878	Mollisol	Kastanozems	NA	NA	NA	5.37	1.55	3	0.59	1.40	0.120	22.0	2.73	0.94	1.53
29	41.9832	-93.6837	Mollisol	Phaeozems	NA	NA	NA	4.50	0.72	3	1.59	1.53	0.160	26.3	3.94	3.80	1.45
30	33.7342	-117.6961	Mollisol	Phaeozems	23.17	10.70	15	3.98	1.10	13	1.21	1.16	0.200	27.3	3.01	1.02	1.63

31	40.0062	-88.2904	Mollisol	Phaeozems	25.22	2.94	15	3.73	0.28	4	1.57	1.45	0.060	25.0	3.73	2.95	1.43
32	38.7441	-92.2000	Mollisol	Phaeozems	26.95	10.04	15	3.60	1.31	4	1.45	1.43	0.110	22.3	3.46	1.20	1.48
33	41.1649	-96.4701	Mollisol	Phaeozems	30.10	3.63	15	3.75	0.60	4	1.26	1.42	0.100	27.3	3.98	2.28	1.48
34	44.3453	-96.8362	Mollisol	Kastanozems	15.90	3.30	5	2.85	0.31	4	1.97	1.40	0.190	24.3	3.28	3.36	1.37
35	44.7143	-93.0898	Mollisol	Chernozems	22.02	11.89	3	2.90	0.67	4	1.72	1.45	0.130	19.0	3.11	2.23	1.48
36	43.1208	-116.7226	Mollisol	Kastanozems	NA	NA	NA	5.70	0.54	4	2.62	0.90	0.090	22.7	3.49	1.59	1.37
37	41.8600	-111.5000	Mollisol	Phaeozems	20.70	5.78	3	2.80	0.45	4	1.72	1.14	0.180	20.7	2.90	3.19	1.34
38	48.3077	-105.1019	Mollisol	Kastanozems	24.71	4.08	15	3.25	0.60	4	1.18	1.28	0.130	23.0	3.39	0.69	1.44
39	35.4455	-111.7719	Mollisol	Kastanozems	38.20	15.74	3	4.35	0.60	1	1.95	NA	NA	31.7	4.43	1.17	1.64
40	35.4386	-111.8036	Mollisol	Kastanozems	33.17	15.74	3	4.08	0.77	1	1.34	NA	NA	31.7	4.43	1.17	1.64
41	40.9482	-97.4875	Mollisol	Kastanozems	NA	NA	NA	3.10	NA	1	1.54	1.33	0.150	20.3	3.25	1.79	1.46
42	40.9338	-97.4587	Mollisol	Kastanozems	NA	NA	NA	2.70	NA	1	1.35	1.43	0.140	20.3	3.25	1.79	1.46
43	41.2688	-97.9470	Mollisol	Kastanozems	NA	NA	NA	1.00	NA	1	0.68	1.47	0.230	5.0	2.45	0.81	1.69
44	41.1657	-96.4303	Mollisol	Phaeozems	NA	NA	NA	3.60	NA	1	6.12	1.40	NA	27.3	3.98	2.28	1.48
45	40.6703	-98.9823	Mollisol	Kastanozems	NA	NA	NA	2.10	NA	1	1.41	1.47	0.190	9.3	3.35	0.56	1.57
46	42.1943	-93.3559	Mollisol	Phaeozems	NA	NA	NA	3.90	NA	1	3.66	NA	NA	27.0	3.87	3.87	1.45
47	40.7591	-98.5382	Mollisol	Kastanozems	NA	NA	NA	2.50	NA	1	2.03	1.31	0.220	9.3	2.83	0.56	1.57
48	41.0655	-101.1027	Mollisol	Kastanozems	NA	NA	NA	1.50	NA	1	0.87	1.58	0.190	4.0	3.01	0.47	1.82
49	41.0584	-101.1027	Mollisol	Kastanozems	NA	NA	NA	2.20	NA	1	1.20	1.53	0.130	4.0	3.01	0.47	1.82
50	41.0656	-101.9581	Mollisol	Kastanozems	NA	NA	NA	1.20	NA	1	0.55	1.67	0.160	17.7	2.62	1.74	1.45
51	42.5378	-72.1715	Spodosol	Podzols	6.37	2.36	15	5.20	3.01	4	6.05	0.89	0.240	4.3	2.68	7.41	1.02
52	45.2041	-68.7402	Spodosol	Podzols	5.97	1.57	15	3.40	1.35	4	8.15	1.23	0.200	10.0	2.68	8.21	0.99
53	45.9459	-90.2723	Spodosol	Podzols	8.01	2.28	15	1.78	0.51	4	1.42	1.26	0.220	9.0	2.68	8.68	1.15
54	45.5598	-84.7138	Spodosol	Podzols	NA	NA	NA	0.33	0.15	4	0.80	1.29	0.190	5.3	2.68	1.66	1.46
55	38.9739	-77.4852	Ultisol	Acrisols	NA	NA	NA	6.37	1.34	3	0.45	1.32	0.150	13.0	2.82	1.24	1.41
56	35.9311	-84.3324	Ultisol	Acrisols	28.08	8.34	15	2.60	0.67	4	1.00	1.41	0.180	18.3	2.82	0.81	1.53
57	29.7381	-82.2188	Ultisol	Acrisols	2.67	0.71	15	0.58	0.21	4	1.08	1.42	0.280	3.0	2.82	2.22	1.42
58	37.9229	-78.2739	Ultisol	Acrisols	19.31	4.77	5	2.33	0.83	4	1.20	NA	NA	17.0	2.82	1.03	1.45
59	35.0662	-83.4370	Ultisol	Acrisols	NA	NA	NA	4.63	0.64	4	1.69	NA	NA	16.3	2.82	1.59	1.46
60	39.0295	-76.8462	Ultisol	Acrisols	11.13	NA	1	0.40	NA	1	0.84	NA	NA	10.3	2.82	1.23	1.38
61	29.9492	-97.9966	Vertisol	Vertisols	34.23	1.26	3	5.18	0.66	4	1.98	NA	NA	2.0	NA	0.70	1.47

Table S2.1: Summary of *in-situ* and GDSE soil information for 61 CO 739 NUS study sites.

ID	Year	Month	Day	Field Number	DOY	Crop (maize =1, soybean =2)	Observed Standing Wet Biomass (kg/m^2)	GrWDRVI
1	2003	6	9	1	160	1	0.0142	0.2341
2	2003	6	14	1	165	1	0.0657	0.2880
3	2003	6	16	1	167	1	0.1203	0.2538
4	2003	6	23	1	174	1	0.5657	0.3779
5	2003	6	23	1	174	1	0.5657	0.4038
6	2003	7	2	1	183	1	1.9377	0.4422
7	2003	7	3	1	184	1	2.1399	0.4314
8	2003	7	10	1	191	1	3.7161	0.5567
9	2003	7	11	1	192	1	3.9499	0.5473
10	2003	7	13	1	194	1	4.4014	0.6025
11	2003	7	14	1	195	1	4.6135	0.6546
12	2003	7	25	1	206	1	5.8348	0.6320
13	2003	7	26	1	207	1	5.8745	0.5521
14	2003	7	28	1	209	1	5.9566	0.6874
15	2003	8	3	1	215	1	6.3009	0.6847
16	2003	8	8	1	220	1	6.6196	0.7314
17	2003	8	10	1	222	1	6.7314	0.6607
18	2003	8	15	1	227	1	6.9519	0.6544
19	2003	8	17	1	229	1	7.0154	0.6797
20	2003	8	24	1	236	1	7.1186	0.7305
21	2003	8	24	1	236	1	7.1186	0.7542
22	2003	8	29	1	241	1	7.0723	0.5934
23	2003	9	4	1	247	1	6.8942	0.5659
24	2003	9	6	1	249	1	6.8098	0.5607
25	2003	9	7	1	250	1	6.7634	0.5881
26	2003	9	15	1	258	1	6.3119	0.4932
27	2003	9	16	1	259	1	6.2474	0.5137
28	2003	9	23	1	266	1	5.7657	0.4029
29	2003	9	25	1	268	1	5.6224	0.4459
30	2004	5	14	1	135	1	0.0001	0.3030
31	2004	5	26	1	147	1	0.0099	0.2260
32	2004	5	27	1	148	1	0.0121	0.2181
33	2004	6	4	1	156	1	0.0447	0.3012
34	2004	6	7	1	159	1	0.0744	0.2508
35	2004	6	13	1	165	1	0.2736	0.3810
36	2004	6	14	1	166	1	0.3358	0.2920
37	2004	6	22	1	174	1	1.2104	0.4486
38	2004	6	23	1	175	1	1.3593	0.4623
39	2004	6	25	1	177	1	1.6765	0.4095
40	2004	6	30	1	182	1	2.5540	0.4751
41	2004	7	4	1	186	1	3.3007	0.6403
42	2004	7	4	1	186	1	3.3007	0.6422
43	2004	7	18	1	200	1	5.4594	0.8630
44	2004	7	18	1	200	1	5.4594	0.7199
45	2004	7	19	1	201	1	5.5565	0.6372
46	2004	7	20	1	202	1	5.6452	0.7349
47	2004	7	27	1	209	1	6.0302	0.7056
48	2004	7	27	1	209	1	6.0302	0.6560
49	2004	8	7	1	220	1	6.3285	0.6927
50	2004	8	8	1	221	1	6.3898	0.7879

51	2004	8	14	1	227	1	6.8078	0.6629
52	2004	8	14	1	227	1	6.8078	0.7046
53	2004	8	21	1	234	1	7.0812	0.6656
54	2004	8	24	1	237	1	7.0732	0.6080
55	2004	8	29	1	242	1	6.9207	0.5006
56	2004	8	30	1	243	1	6.8723	0.6102
57	2004	9	6	1	250	1	6.4053	0.5378
58	2004	9	9	1	253	1	6.1544	0.4627
59	2004	9	13	1	257	1	5.7871	0.4812
60	2004	9	16	1	260	1	5.4913	0.4295
61	2004	9	24	1	268	1	4.6434	0.3402
62	2004	9	25	1	269	1	4.5335	0.3730
63	2004	9	29	1	273	1	4.0903	0.3232
64	2005	5	20	1	140	1	0.0030	0.2395
65	2005	5	23	1	143	1	0.0059	0.2315
66	2005	5	27	1	147	1	0.0099	0.2086
67	2005	6	8	1	159	1	0.0695	0.2297
68	2005	6	17	1	168	1	0.4827	0.3020
69	2005	6	21	1	172	1	0.8833	0.3204
70	2005	6	22	1	173	1	1.0093	0.3548
71	2005	6	28	1	179	1	2.0085	0.4625
72	2005	7	1	1	182	1	2.6499	0.5245
73	2005	7	5	1	186	1	3.5297	0.6603
74	2005	7	19	1	200	1	5.6120	0.6196
75	2005	7	23	1	204	1	6.0460	0.6211
76	2005	7	24	1	205	1	6.1454	0.5464
77	2005	7	28	1	209	1	6.4655	0.7880
78	2005	7	28	1	209	1	6.4655	0.7443
79	2005	8	8	1	220	1	6.3918	0.8040
80	2005	8	9	1	221	1	6.3643	0.7698
81	2005	8	18	1	230	1	6.4063	0.6796
82	2005	8	18	1	230	1	6.4063	0.6700
83	2005	8	27	1	239	1	6.2754	0.7065
84	2005	8	28	1	240	1	6.2360	0.5700
85	2005	8	31	1	243	1	6.0920	0.6162
86	2005	9	3	1	246	1	5.9121	0.5437
87	2005	9	9	1	252	1	5.4601	0.5195
88	2005	9	10	1	253	1	5.3746	0.4308
89	2005	9	16	1	259	1	4.8131	0.4055
90	2005	9	19	1	262	1	4.5067	0.3055
91	2005	9	26	1	269	1	3.7456	0.3327
92	2005	9	27	1	270	1	3.6331	0.3295
93	2005	10	2	1	275	1	3.0632	0.2827
94	2006	5	19	1	139	1	-0.0297	0.1685
95	2006	5	25	1	145	1	-0.0497	0.2069
96	2006	5	28	1	148	1	-0.0201	0.1867
97	2006	6	6	1	157	1	0.3309	0.2795
98	2006	6	9	1	160	1	0.5337	0.2743
99	2006	6	13	1	164	1	0.9028	0.3510
100	2006	6	13	1	164	1	0.9028	0.2862

101	2006	6	20	1	171	1	2.1717	0.4411
102	2006	6	22	1	173	1	2.6630	0.5064
103	2006	7	1	1	182	1	4.7143	0.5563
104	2006	7	1	1	182	1	4.7143	0.5655
105	2006	7	6	1	187	1	5.3059	0.6522
106	2006	7	6	1	187	1	5.3059	0.4973
107	2006	7	15	1	196	1	5.6367	0.6933
108	2006	7	17	1	198	1	5.8326	0.6961
109	2006	7	20	1	201	1	6.1632	0.7199
110	2006	7	26	1	207	1	6.6937	0.6657
111	2006	7	29	1	210	1	6.7856	0.6482
112	2006	8	4	1	216	1	6.6857	0.7076
113	2006	8	5	1	217	1	6.6737	0.6857
114	2006	8	9	1	221	1	6.6727	0.6417
115	2006	8	14	1	226	1	6.6571	0.7834
116	2006	8	14	1	226	1	6.6571	0.6831
117	2006	8	23	1	235	1	6.6230	0.7158
118	2006	8	29	1	241	1	7.3285	0.6134
119	2006	8	30	1	242	1	7.4621	0.6097
120	2006	9	12	1	255	1	5.2796	0.5252
121	2006	9	13	1	256	1	4.5639	0.3806
122	2006	9	17	1	260	1	0.9844	0.3621
123	2007	5	17	1	137	1	0.0014	0.2153
124	2007	5	25	1	145	1	0.0366	0.2558
125	2007	6	7	1	158	1	0.4657	0.2564
126	2007	6	9	1	160	1	0.6425	0.3316
127	2007	6	16	1	167	1	1.6994	0.4618
128	2007	6	16	1	167	1	1.6994	0.4638
129	2007	6	20	1	171	1	2.7227	0.4299
130	2007	6	20	1	171	1	2.7227	0.5661
131	2007	6	30	1	181	1	5.4796	0.6388
132	2007	6	30	1	181	1	5.4796	0.5223
133	2007	7	4	1	185	1	6.0484	0.6777
134	2007	7	11	1	192	1	6.5392	0.7139
135	2007	7	13	1	194	1	6.6473	0.5690
136	2007	7	16	1	197	1	6.9077	0.6203
137	2007	7	20	1	201	1	7.5190	0.7427
138	2007	8	3	1	215	1	8.4266	0.7583
139	2007	8	4	1	216	1	8.3850	0.6563
140	2007	8	9	1	221	1	8.0865	0.6321
141	2007	8	10	1	222	1	8.0149	0.8552
142	2007	8	13	1	225	1	7.7918	0.7205
143	2007	8	14	1	226	1	7.7176	0.7158
144	2007	8	21	1	233	1	7.2583	0.7513
145	2007	8	28	1	240	1	6.8572	0.6983
146	2007	8	30	1	242	1	6.7389	0.6546
147	2007	9	2	1	245	1	6.5490	0.6447
148	2007	9	8	1	251	1	6.0985	0.5598
149	2007	9	11	1	254	1	5.8361	0.5083
150	2007	9	14	1	257	1	5.5544	0.4367

151	2007	9	17	1	260	1	5.2580	0.4080
152	2007	9	22	1	265	1	4.7431	0.3819
153	2008	5	12	1	133	1	0.0032	0.2008
154	2008	5	15	1	136	1	0.0059	0.2480
155	2008	5	16	1	137	1	0.0066	0.2379
156	2008	5	17	1	138	1	0.0072	0.2933
157	2008	5	30	1	151	1	0.0197	0.3693
158	2008	6	6	1	158	1	0.1215	0.2591
159	2008	6	6	1	158	1	0.1215	0.4016
160	2008	6	13	1	165	1	0.4350	0.3162
161	2008	6	16	1	168	1	0.7172	0.3786
162	2008	6	20	1	172	1	1.4044	0.3930
163	2008	6	27	1	179	1	3.3107	0.5412
164	2008	7	2	1	184	1	4.6729	0.5467
165	2008	7	5	1	187	1	5.2829	0.5122
166	2008	7	10	1	192	1	6.0142	0.5479
167	2008	7	11	1	193	1	6.1372	0.6607
168	2008	7	15	1	197	1	6.6287	0.6740
169	2008	7	20	1	202	1	7.3795	0.6614
170	2008	7	22	1	204	1	7.6632	0.7143
171	2008	8	2	1	215	1	6.9763	0.6587
172	2008	8	3	1	216	1	6.8592	0.7607
173	2008	8	7	1	220	1	6.9166	0.6761
174	2008	8	12	1	225	1	7.6414	0.7182
175	2008	8	23	1	236	1	7.7514	0.6246
176	2008	8	26	1	239	1	7.6787	0.6999
177	2008	9	1	1	245	1	7.5914	0.5986
178	2008	9	4	1	248	1	7.5449	0.5137
179	2008	9	17	1	261	1	6.9029	0.4232
180	2008	9	20	1	264	1	6.6249	0.4193
181	2008	9	26	1	270	1	5.9702	0.3568
182	2008	9	27	1	271	1	5.8518	0.3688
183	2008	10	1	1	275	1	5.3630	0.3944
184	2008	10	1	1	275	1	5.3630	0.3619
185	2009	5	6	1	126	1	0.0012	0.2044
186	2009	5	9	1	129	1	0.0048	0.3441
187	2009	5	9	1	129	1	0.0048	0.1871
188	2009	5	18	1	138	1	0.0157	0.2354
189	2009	5	22	1	142	1	0.0216	0.2192
190	2009	5	29	1	149	1	0.1043	0.2607
191	2009	5	29	1	149	1	0.1043	0.2516
192	2009	6	3	1	154	1	0.2781	0.2463
193	2009	6	4	1	155	1	0.3210	0.2583
194	2009	6	23	1	174	1	3.6159	0.6315
195	2009	6	25	1	176	1	4.2540	0.5260
196	2009	6	30	1	181	1	5.0755	0.5956
197	2009	7	8	1	189	1	6.0977	0.6327
198	2009	7	9	1	190	1	6.2157	0.7121
199	2009	7	14	1	195	1	6.4540	0.7445
200	2009	7	23	1	204	1	6.5781	0.8890

201	2009	7	25	1	206	1	6.7844	0.7442
202	2009	7	31	1	212	1	7.6585	0.7325
203	2009	8	2	1	214	1	7.9438	0.6470
204	2009	8	6	1	218	1	8.3569	0.6794
205	2009	8	8	1	220	1	8.4707	0.7749
206	2009	8	13	1	225	1	8.4861	0.8009
207	2009	8	14	1	226	1	8.4454	0.7182
208	2009	8	24	1	236	1	7.7446	0.7885
209	2009	8	24	1	236	1	7.7446	0.7323
210	2009	8	29	1	241	1	7.5281	0.6161
211	2009	9	6	1	249	1	7.2781	0.5925
212	2009	9	19	1	262	1	6.5190	0.4140
213	2009	9	20	1	263	1	6.4485	0.4076
214	2010	5	5	1	125	1	-0.0024	0.1842
215	2010	5	9	1	129	1	-0.0113	0.2375
216	2010	5	14	1	134	1	-0.0170	0.2129
217	2010	5	28	1	148	1	0.0459	0.2708
218	2010	6	3	1	154	1	0.1949	0.2644
219	2010	6	21	1	172	1	2.6735	0.4643
220	2010	6	22	1	173	1	2.9054	0.4916
221	2010	6	26	1	177	1	3.7858	0.5151
222	2010	7	1	1	182	1	4.5827	0.5435
223	2010	7	6	1	187	1	5.0019	0.6288
224	2010	7	10	1	191	1	5.1768	0.6755
225	2010	7	14	1	195	1	5.3844	0.6325
226	2010	7	19	1	200	1	5.8770	0.7341
227	2010	7	22	1	203	1	6.1989	0.6380
228	2010	7	27	1	208	1	6.5231	0.6086
229	2010	7	31	1	212	1	6.4746	0.7310
230	2010	8	3	1	215	1	6.4258	0.6329
231	2010	8	8	1	220	1	6.5904	0.6514
232	2010	8	11	1	223	1	6.6941	0.8213
233	2010	8	15	1	227	1	6.6517	0.5898
234	2010	8	16	1	228	1	6.6087	0.7755
235	2010	8	22	1	234	1	6.1415	0.6411
236	2010	8	25	1	237	1	5.8096	0.6097
237	2010	8	29	1	241	1	5.3143	0.5521
238	2011	5	30	1	150	1	0.0045	0.2269
239	2011	5	31	1	151	1	0.0055	0.2100
240	2011	6	6	1	157	1	0.0107	0.2071
241	2011	6	18	1	169	1	0.1998	0.3204
242	2011	6	25	1	176	1	0.6234	0.3199
243	2011	6	27	1	178	1	0.8151	0.3821
244	2011	6	29	1	180	1	1.0519	0.3401
245	2011	7	4	1	185	1	1.9021	0.5142
246	2011	7	8	1	189	1	2.8855	0.4458
247	2011	7	18	1	199	1	4.2897	0.6265
248	2011	7	19	1	200	1	4.2728	0.5421
249	2011	7	20	1	201	1	4.2513	0.7162
250	2011	7	26	1	207	1	4.5111	0.6249

251	2011	8	3	1	215	1	6.0571	0.7659
252	2011	8	3	1	215	1	6.0571	0.7836
253	2011	8	9	1	221	1	6.4408	0.7268
254	2011	8	12	1	224	1	6.4579	0.8609
255	2011	8	18	1	230	1	6.4300	0.6696
256	2011	8	19	1	231	1	6.4221	0.7865
257	2011	8	24	1	236	1	6.3880	0.6770
258	2011	8	25	1	237	1	6.3839	0.6724
259	2011	9	1	1	244	1	6.3578	0.6494
260	2011	9	4	1	247	1	6.3328	0.6797
261	2011	9	6	1	249	1	6.3060	0.6636
262	2011	9	10	1	253	1	6.2183	0.6501
263	2011	9	19	1	262	1	5.8433	0.5168
264	2011	9	20	1	263	1	5.7875	0.5493
265	2011	9	22	1	265	1	5.6681	0.5433
266	2011	9	26	1	269	1	5.3995	0.4637
267	2011	10	1	1	274	1	5.0129	0.4303
268	2011	10	3	1	276	1	4.8458	0.4093
269	2012	5	5	1	126	1	0.0002	0.2812
270	2012	5	10	1	131	1	0.0076	0.2248
271	2012	5	14	1	135	1	0.0245	0.2068
272	2012	5	16	1	137	1	0.0352	0.2127
273	2012	5	17	1	138	1	0.0406	0.1975
274	2012	5	28	1	149	1	0.3507	0.3201
275	2012	5	28	1	149	1	0.3507	0.3280
276	2012	6	4	1	156	1	0.8039	0.4012
277	2012	6	4	1	156	1	0.8039	0.3511
278	2012	6	11	1	163	1	1.7223	0.4927
279	2012	6	12	1	164	1	1.9494	0.4509
280	2012	6	18	1	170	1	3.5064	0.5408
281	2012	6	24	1	176	1	4.3145	0.6611
282	2012	6	26	1	178	1	4.4159	0.5638
283	2012	6	27	1	179	1	4.4667	0.6519
284	2012	7	6	1	188	1	5.5607	0.7058
285	2012	7	10	1	192	1	6.3633	0.6079
286	2012	7	13	1	195	1	6.6639	0.7111
287	2012	7	17	1	199	1	6.5113	0.7457
288	2012	7	22	1	204	1	6.2296	0.6384
289	2012	7	26	1	208	1	6.2299	0.5379
290	2012	7	29	1	211	1	6.2854	0.6099
291	2012	8	2	1	215	1	6.3535	0.6243
292	2012	8	4	1	217	1	6.3616	0.5314
293	2012	8	5	1	218	1	6.3547	0.4382
294	2012	8	15	1	228	1	5.8971	0.4566
295	2012	8	21	1	234	1	5.5771	0.4611
296	2012	8	27	1	240	1	5.2967	0.3604
297	2013	5	15	1	135	1	0.0008	0.2460
298	2013	5	23	1	143	1	0.0115	0.3129
299	2013	5	27	1	147	1	0.0269	0.3123
300	2013	5	31	1	151	1	0.0621	0.2857

301	2013	6	2	1	153	1	0.0898	0.3042
302	2013	6	3	1	154	1	0.1053	0.2748
303	2013	6	13	1	164	1	0.3942	0.3151
304	2013	6	14	1	165	1	0.5000	0.3613
305	2013	6	22	1	173	1	1.9206	0.3716
306	2013	6	28	1	179	1	2.9443	0.5345
307	2013	7	4	1	185	1	3.6886	0.5788
308	2013	7	9	1	190	1	4.2773	0.6434
309	2013	7	18	1	199	1	5.5428	0.6327
310	2013	7	22	1	203	1	5.9403	0.6116
311	2013	7	23	1	204	1	6.0125	0.5986
312	2013	8	17	1	229	1	6.0131	0.7582
313	2013	8	19	1	231	1	6.0136	0.7758
314	2013	8	23	1	235	1	6.0114	0.5968
315	2013	8	26	1	238	1	6.0173	0.7028
316	2003	6	9	2	160	1	0.0049	0.2362
317	2003	6	9	2	160	1	0.0049	0.3367
318	2003	6	14	2	165	1	0.0624	0.3207
319	2003	6	16	2	167	1	0.1382	0.2755
320	2003	6	23	2	174	1	0.8006	0.4571
321	2003	6	23	2	174	1	0.8006	0.4184
322	2003	7	2	2	183	1	2.7231	0.4854
323	2003	7	3	2	184	1	2.9681	0.4044
324	2003	7	11	2	192	1	4.6544	0.5867
325	2003	7	13	2	194	1	4.9685	0.6219
326	2003	7	14	2	195	1	5.1110	0.5391
327	2003	7	25	2	206	1	6.2933	0.6912
328	2003	7	26	2	207	1	6.3959	0.4683
329	2003	7	28	2	209	1	6.6108	0.6982
330	2003	8	3	2	215	1	7.3258	0.6054
331	2003	8	8	2	220	1	7.9875	0.6643
332	2003	8	10	2	222	1	8.2581	0.6007
333	2003	8	15	2	227	1	8.8827	0.6160
334	2003	8	17	2	229	1	9.0906	0.6494
335	2003	8	24	2	236	1	9.4833	0.6235
336	2003	8	24	2	236	1	9.4833	0.5790
337	2003	8	29	2	241	1	9.3938	0.5168
338	2003	9	4	2	247	1	8.9842	0.4947
339	2003	9	6	2	249	1	8.7977	0.4638
340	2003	9	7	2	250	1	8.6981	0.4358
341	2005	5	20	2	140	1	-0.0111	0.2373
342	2005	5	23	2	143	1	-0.0117	0.2176
343	2005	5	27	2	147	1	-0.0032	0.2712
344	2005	5	28	2	148	1	0.0011	0.2575
345	2005	6	8	2	159	1	0.1729	0.2642
346	2005	6	17	2	168	1	0.8001	0.3480
347	2005	6	21	2	172	1	1.3430	0.4189
348	2005	6	22	2	173	1	1.5117	0.3892
349	2005	6	28	2	179	1	2.7775	0.5404
350	2005	7	1	2	182	1	3.4557	0.5595

351	2005	7	5	2	186	1	4.2280	0.6503
352	2005	7	7	2	188	1	4.5057	0.7392
353	2005	7	19	2	200	1	5.7477	0.5785
354	2005	7	23	2	204	1	6.2061	0.5810
355	2005	7	24	2	205	1	6.3018	0.5513
356	2005	7	28	2	209	1	6.5490	0.6651
357	2005	7	28	2	209	1	6.5490	0.6492
358	2005	8	8	2	220	1	6.6195	0.6555
359	2005	8	9	2	221	1	6.6421	0.6690
360	2005	8	18	2	230	1	6.8858	0.7100
361	2005	8	18	2	230	1	6.8858	0.6495
362	2005	8	27	2	239	1	6.9131	0.6294
363	2005	8	28	2	240	1	6.8888	0.5259
364	2005	8	31	2	243	1	6.7721	0.5948
365	2005	9	3	2	246	1	6.5821	0.4819
366	2005	9	9	2	252	1	6.0066	0.4156
367	2005	9	10	2	253	1	5.8910	0.4256
368	2005	9	16	2	259	1	5.1227	0.4180
369	2005	9	19	2	262	1	4.7125	0.3564
370	2007	5	17	2	137	1	0.0034	0.2531
371	2007	5	25	2	145	1	0.0438	0.3017
372	2007	6	9	2	160	1	0.5440	0.3262
373	2007	6	16	2	167	1	1.2516	0.4304
374	2007	6	20	2	171	1	1.8996	0.4332
375	2007	6	20	2	171	1	1.8996	0.5309
376	2007	6	30	2	181	1	4.8505	0.5876
377	2007	6	30	2	181	1	4.8505	0.5212
378	2007	7	4	2	185	1	5.2226	0.6207
379	2007	7	11	2	192	1	5.8544	0.6280
380	2007	7	13	2	194	1	6.2791	0.6450
381	2007	7	16	2	197	1	7.0098	0.5967
382	2007	7	20	2	201	1	7.8330	0.6642
383	2007	7	26	2	207	1	8.5960	0.6355
384	2007	8	4	2	216	1	9.1317	0.5834
385	2007	8	10	2	222	1	9.0101	0.6148
386	2007	8	13	2	225	1	8.8040	0.6047
387	2007	8	14	2	226	1	8.7208	0.6198
388	2007	8	21	2	233	1	8.0672	0.6760
389	2007	8	28	2	240	1	7.5059	0.5817
390	2007	8	30	2	242	1	7.3625	0.6079
391	2007	9	2	2	245	1	7.1511	0.5318
392	2007	9	8	2	251	1	6.7063	0.4523
393	2007	9	11	2	254	1	6.4539	0.4282
394	2007	9	14	2	257	1	6.1714	0.3965
395	2007	9	17	2	260	1	5.8624	0.3590
396	2007	9	22	2	265	1	5.3050	0.3847
397	2007	9	27	2	270	1	4.7193	0.3332
398	2009	5	9	2	129	1	0.0056	0.2681
399	2009	5	9	2	129	1	0.0056	0.2012
400	2009	5	18	2	138	1	0.0159	0.1949

401	2009	5	22	2	142	1	0.0148	0.2041
402	2009	5	29	2	149	1	0.0715	0.2433
403	2009	6	3	2	154	1	0.2162	0.2475
404	2009	6	4	2	155	1	0.2475	0.2506
405	2009	6	23	2	174	1	3.7708	0.5688
406	2009	6	25	2	176	1	4.3396	0.6118
407	2009	6	28	2	179	1	4.8900	0.6709
408	2009	6	30	2	181	1	5.1955	0.6757
409	2009	7	8	2	189	1	6.6528	0.6257
410	2009	7	9	2	190	1	6.8003	0.7956
411	2009	7	14	2	195	1	7.2682	0.8181
412	2009	7	19	2	200	1	7.5344	0.7283
413	2009	7	23	2	204	1	7.8307	0.8416
414	2009	7	31	2	212	1	8.5778	0.7492
415	2009	8	2	2	214	1	8.6980	0.7284
416	2009	8	6	2	218	1	8.8259	0.7798
417	2009	8	8	2	220	1	8.8373	0.8025
418	2009	8	13	2	225	1	8.7296	0.7167
419	2009	8	14	2	226	1	8.6901	0.6846
420	2009	8	24	2	236	1	8.3622	0.7310
421	2009	8	24	2	236	1	8.3622	0.7382
422	2009	8	29	2	241	1	8.2928	0.5604
423	2009	8	30	2	242	1	8.2728	0.6456
424	2009	9	6	2	249	1	7.9916	0.5549
425	2009	9	19	2	262	1	6.9989	0.3791
426	2009	9	20	2	263	1	6.9099	0.4446
427	2010	5	14	2	134	1	0.0027	0.2194
428	2010	5	22	2	142	1	0.0148	0.2492
429	2010	6	17	2	168	1	1.1249	0.3569
430	2010	6	21	2	172	1	1.5130	0.3782
431	2010	6	22	2	173	1	1.6067	0.4335
432	2010	6	26	2	177	1	1.9547	0.4276
433	2010	7	1	2	182	1	2.4428	0.4322
434	2010	7	10	2	191	1	3.9981	0.5912
435	2010	7	14	2	195	1	4.7507	0.5590
436	2010	7	19	2	200	1	5.5207	0.6526
437	2010	7	22	2	203	1	5.8776	0.5873
438	2010	7	27	2	208	1	6.2834	0.5951
439	2010	7	31	2	212	1	6.4276	0.5413
440	2010	8	3	2	215	1	6.4464	0.5929
441	2010	8	8	2	220	1	6.3942	0.6180
442	2010	8	11	2	223	1	6.3617	0.7231
443	2010	8	15	2	227	1	6.3453	0.5953
444	2010	8	22	2	234	1	6.2976	0.6014
445	2010	8	25	2	237	1	6.2301	0.6133
446	2010	8	29	2	241	1	6.0695	0.5349
447	2010	9	3	2	246	1	5.7794	0.5510
448	2010	9	7	2	250	1	5.5049	0.5262
449	2011	5	30	2	150	1	0.0072	0.1922
450	2011	5	31	2	151	1	0.0083	0.2144

451	2011	6	6	2	157	1	0.0086	0.1916
452	2011	6	7	2	158	1	0.0139	0.2426
453	2011	6	18	2	169	1	0.5082	0.3607
454	2011	6	25	2	176	1	1.0423	0.4897
455	2011	6	27	2	178	1	1.2559	0.4055
456	2011	6	29	2	180	1	1.5406	0.3711
457	2011	7	4	2	185	1	2.6856	0.5086
458	2011	7	8	2	189	1	3.8151	0.5959
459	2011	7	18	2	199	1	5.0942	0.6518
460	2011	7	19	2	200	1	5.1523	0.6277
461	2011	7	20	2	201	1	5.2320	0.7021
462	2011	7	26	2	207	1	6.0969	0.6874
463	2011	8	3	2	215	1	6.5961	0.8568
464	2011	8	3	2	215	1	6.5961	0.7557
465	2011	8	9	2	221	1	6.4575	0.6819
466	2011	8	12	2	224	1	6.4893	0.7991
467	2011	8	18	2	230	1	6.6813	0.6572
468	2011	8	19	2	231	1	6.7129	0.7555
469	2011	8	25	2	237	1	6.8212	0.6401
470	2011	9	1	2	244	1	6.7733	0.6359
471	2011	9	4	2	247	1	6.6975	0.6366
472	2011	9	6	2	249	1	6.6289	0.6947
473	2011	9	10	2	253	1	6.4513	0.5682
474	2011	9	19	2	262	1	5.8982	0.5320
475	2011	9	20	2	263	1	5.8274	0.5169
476	2011	9	26	2	269	1	5.3785	0.4790
477	2011	10	1	2	274	1	4.9833	0.4459
478	2011	10	3	2	276	1	4.8227	0.4033
479	2012	5	5	2	126	1	0.0007	0.2609
480	2012	5	10	2	131	1	0.0069	0.2168
481	2012	5	14	2	135	1	0.0230	0.1862
482	2012	5	16	2	137	1	0.0384	0.2255
483	2012	5	17	2	138	1	0.0486	0.1955
484	2012	5	28	2	149	1	0.4121	0.3467
485	2012	5	28	2	149	1	0.4121	0.3244
486	2012	6	4	2	156	1	0.9587	0.3803
487	2012	6	4	2	156	1	0.9587	0.3355
488	2012	6	11	2	163	1	1.8605	0.4483
489	2012	6	12	2	164	1	2.0860	0.4387
490	2012	6	18	2	170	1	3.7875	0.4613
491	2012	6	24	2	176	1	4.6225	0.5671
492	2012	6	26	2	178	1	4.7600	0.5939
493	2012	6	27	2	179	1	4.8385	0.6315
494	2012	7	6	2	188	1	6.2283	0.6455
495	2012	7	10	2	192	1	6.8497	0.6326
496	2012	7	13	2	195	1	6.8656	0.6642
497	2012	7	17	2	199	1	6.5693	0.6038
498	2012	7	22	2	204	1	6.5395	0.6479
499	2012	7	26	2	208	1	6.7559	0.6057
500	2012	7	29	2	211	1	6.9082	0.6142

501	2012	8	2	2	215	1	7.0494	0.5676
502	2012	8	4	2	217	1	7.0833	0.5331
503	2012	8	5	2	218	1	7.0896	0.5282
504	2012	8	15	2	228	1	6.6870	0.5113
505	2012	8	19	2	232	1	6.3016	0.4375
506	2012	8	21	2	234	1	6.0952	0.4257
507	2012	8	27	2	240	1	5.5558	0.4086
508	2012	8	29	2	242	1	5.4155	0.3838
509	2012	8	30	2	243	1	5.3517	0.3555
510	2012	9	5	2	249	1	5.0379	0.2917
511	2012	9	8	2	252	1	4.9110	0.3168
512	2013	5	15	2	135	1	0.0000	0.2009
513	2013	5	23	2	143	1	0.0100	0.3129
514	2013	5	27	2	147	1	0.0293	0.2577
515	2013	5	31	2	151	1	0.0675	0.2729
516	2013	6	2	2	153	1	0.0958	0.2250
517	2013	6	3	2	154	1	0.1123	0.2455
518	2013	6	13	2	164	1	0.3657	0.2832
519	2013	6	14	2	165	1	0.4226	0.3288
520	2013	6	22	2	173	1	1.8810	0.4079
521	2013	6	28	2	179	1	3.5703	0.5366
522	2013	6	29	2	180	1	3.7654	0.4795
523	2013	7	4	2	185	1	4.3178	0.5239
524	2013	7	9	2	190	1	4.4218	0.6579
525	2013	7	16	2	197	1	5.3211	0.6520
526	2013	7	18	2	199	1	5.7599	0.6806
527	2013	7	23	2	204	1	6.5457	0.6546
528	2013	8	7	2	219	1	6.4347	0.6197
529	2013	8	10	2	222	1	6.7095	0.5603
530	2013	8	17	2	229	1	6.9161	0.7253
531	2013	8	26	2	238	1	6.4687	0.6490
532	2013	8	30	2	242	1	6.2736	0.5899
533	2013	9	2	2	245	1	6.1469	0.5858
534	2013	9	6	2	249	1	5.9771	0.5052
535	2013	9	9	2	252	1	5.8304	0.4296
536	2003	6	9	3	160	1	0.0197	0.3446
537	2003	6	14	3	165	1	0.0888	0.2817
538	2003	6	16	3	167	1	0.1669	0.2969
539	2003	6	23	3	174	1	0.7986	0.3802
540	2003	6	23	3	174	1	0.7986	0.3902
541	2003	6	26	3	177	1	1.2313	0.3533
542	2003	7	2	3	183	1	2.2682	0.4412
543	2003	7	11	3	192	1	3.8191	0.4689
544	2003	7	13	3	194	1	4.0646	0.4788
545	2003	7	14	3	195	1	4.1631	0.5877
546	2003	7	25	3	206	1	4.5673	0.4735
547	2003	7	26	3	207	1	4.5972	0.4539
548	2003	8	3	3	215	1	4.9179	0.5803
549	2003	8	8	3	220	1	5.1488	0.3940
550	2003	8	10	3	222	1	5.2265	0.4219

551	2003	8	17	3	229	1	5.2963	0.4223
552	2003	8	20	3	232	1	5.1742	0.3914
553	2003	8	24	3	236	1	4.8288	0.3968
554	2003	8	24	3	236	1	4.8288	0.4422
555	2003	8	29	3	241	1	4.1705	0.3729
556	2003	9	4	3	247	1	3.2039	0.3846
557	2005	5	16	3	136	1	0.0149	0.2593
558	2005	5	20	3	140	1	0.0190	0.2634
559	2005	5	28	3	148	1	-0.0097	0.2719
560	2005	6	6	3	157	1	0.1248	0.4092
561	2005	6	8	3	159	1	0.2295	0.2433
562	2005	6	16	3	167	1	0.9782	0.3501
563	2005	6	17	3	168	1	1.0967	0.3070
564	2005	6	21	3	172	1	1.5922	0.3548
565	2005	6	22	3	173	1	1.7173	0.3905
566	2005	6	28	3	179	1	2.4077	0.5298
567	2005	7	1	3	182	1	2.6703	0.4721
568	2005	7	5	3	186	1	2.9222	0.5019
569	2005	7	5	3	186	1	2.9222	0.4907
570	2005	7	19	3	200	1	3.9885	0.5510
571	2005	7	23	3	204	1	4.4226	0.4722
572	2005	7	24	3	205	1	4.5197	0.3655
573	2005	7	28	3	209	1	4.8099	0.5552
574	2005	7	28	3	209	1	4.8099	0.5314
575	2005	8	8	3	220	1	4.8682	0.5283
576	2005	8	9	3	221	1	4.8764	0.6139
577	2005	8	18	3	230	1	5.0334	0.6858
578	2005	8	18	3	230	1	5.0334	0.7048
579	2005	8	27	3	239	1	4.8631	0.6498
580	2005	8	28	3	240	1	4.8240	0.4577
581	2005	8	31	3	243	1	4.6907	0.5388
582	2005	9	3	3	246	1	4.5395	0.5389
583	2005	9	9	3	252	1	4.2161	0.4625
584	2005	9	10	3	253	1	4.1622	0.3720
585	2005	9	16	3	259	1	3.8413	0.3765
586	2005	9	19	3	262	1	3.6821	0.3425
587	2005	9	26	3	269	1	3.3122	0.3281
588	2007	5	17	3	137	1	0.0024	0.2017
589	2007	5	18	3	138	1	0.0048	0.2821
590	2007	5	25	3	145	1	0.0280	0.3348
591	2007	6	7	3	158	1	0.2089	0.3181
592	2007	6	16	3	167	1	0.8946	0.3823
593	2007	6	16	3	167	1	0.8946	0.3758
594	2007	6	20	3	171	1	1.4571	0.3769
595	2007	6	20	3	171	1	1.4571	0.4355
596	2007	6	30	3	181	1	3.3049	0.4538
597	2007	7	11	3	192	1	4.2725	0.5729
598	2007	7	13	3	194	1	4.4264	0.5807
599	2007	7	16	3	197	1	4.7090	0.4325
600	2007	7	20	3	201	1	5.1310	0.6587

601	2007	7	26	3	207	1	5.7039	0.5203
602	2007	8	2	3	214	1	6.0068	0.5152
603	2007	8	4	3	216	1	5.9867	0.6071
604	2007	8	10	3	222	1	5.7261	0.7102
605	2007	8	12	3	224	1	5.6040	0.5514
606	2007	8	13	3	225	1	5.5416	0.6003
607	2007	8	14	3	226	1	5.4800	0.5952
608	2007	8	21	3	233	1	5.1024	0.6689
609	2007	8	28	3	240	1	4.7626	0.5646
610	2007	8	30	3	242	1	4.6597	0.5810
611	2007	9	2	3	245	1	4.4966	0.5056
612	2007	9	8	3	251	1	4.1450	0.5235
613	2007	9	11	3	254	1	3.9602	0.4709
614	2007	9	14	3	257	1	3.7718	0.4025
615	2009	5	9	3	129	1	0.0009	0.2960
616	2009	5	9	3	129	1	0.0009	0.2546
617	2009	5	18	3	138	1	0.0085	0.2526
618	2009	5	22	3	142	1	0.0161	0.2412
619	2009	5	29	3	149	1	0.0743	0.2711
620	2009	5	29	3	149	1	0.0743	0.2325
621	2009	6	3	3	154	1	0.2091	0.2535
622	2009	6	23	3	174	1	3.7505	0.5408
623	2009	6	25	3	176	1	4.3881	0.5449
624	2009	6	28	3	179	1	4.9576	0.5282
625	2009	6	30	3	181	1	5.1814	0.5874
626	2009	7	6	3	187	1	5.7967	0.5331
627	2009	7	8	3	189	1	5.9160	0.6058
628	2009	7	12	3	193	1	5.9023	0.6888
629	2009	7	14	3	195	1	5.8591	0.5718
630	2009	7	23	3	204	1	6.4201	0.7094
631	2009	7	23	3	204	1	6.4201	0.5962
632	2009	7	31	3	212	1	7.0490	0.5570
633	2009	8	2	3	214	1	7.0837	0.5313
634	2009	8	6	3	218	1	7.0041	0.6206
635	2009	8	8	3	220	1	6.9038	0.6411
636	2009	8	13	3	225	1	6.6437	0.6408
637	2009	8	24	3	236	1	6.5925	0.5393
638	2009	9	6	3	249	1	5.9342	0.4091
639	2011	5	17	3	137	1	-0.0003	0.2102
640	2011	5	23	3	143	1	0.0010	0.2108
641	2011	5	30	3	150	1	0.0086	0.2469
642	2011	5	31	3	151	1	0.0107	0.3098
643	2011	6	6	3	157	1	0.0341	0.2381
644	2011	6	7	3	158	1	0.0402	0.2406
645	2011	6	15	3	166	1	0.1386	0.3813
646	2011	6	18	3	169	1	0.2153	0.3112
647	2011	6	27	3	178	1	0.9963	0.3421
648	2011	6	29	3	180	1	1.3940	0.3748
649	2011	7	4	3	185	1	2.6442	0.4955
650	2011	7	8	3	189	1	3.4764	0.4949

651	2011	7	18	3	199	1	3.9639	0.5238
652	2011	7	19	3	200	1	3.9890	0.5840
653	2011	7	20	3	201	1	4.0192	0.6595
654	2011	8	3	3	215	1	5.2761	0.7360
655	2011	8	9	3	221	1	5.4756	0.5785
656	2011	8	12	3	224	1	5.4036	0.6798
657	2011	8	18	3	230	1	5.1691	0.5924
658	2011	8	19	3	231	1	5.1307	0.6727
659	2011	8	25	3	237	1	4.8985	0.5830
660	2011	8	28	3	240	1	4.7743	0.5525
661	2011	9	1	3	244	1	4.5982	0.5197
662	2011	9	4	3	247	1	4.4596	0.4774
663	2011	9	6	3	249	1	4.3645	0.4447
664	2011	9	10	3	253	1	4.1691	0.4137
665	2011	9	19	3	262	1	3.7132	0.3626
666	2011	9	20	3	263	1	3.6616	0.3375
667	2011	9	26	3	269	1	3.3501	0.3319
668	2011	9	29	3	272	1	3.1936	0.2890
669	2013	5	27	3	147	1	0.0029	0.2983
670	2013	5	31	3	151	1	0.0220	0.2847
671	2013	6	3	3	154	1	0.0782	0.3532
672	2013	6	13	3	164	1	0.4198	0.2916
673	2013	6	14	3	165	1	0.4064	0.3020
674	2013	6	28	3	179	1	1.5774	0.4025
675	2013	7	4	3	185	1	2.7877	0.4436
676	2013	7	9	3	190	1	3.6937	0.5307
677	2013	7	18	3	199	1	4.6783	0.6995
678	2013	7	20	3	201	1	4.7993	0.4304
679	2013	7	23	3	204	1	4.9782	0.5403
680	2013	8	7	3	219	1	6.1104	0.5491
681	2013	8	12	3	224	1	5.9754	0.6153
682	2013	8	23	3	235	1	5.5129	0.5157
683	2013	8	30	3	242	1	5.1589	0.4150
684	2013	9	2	3	245	1	4.9363	0.4057
685	2013	9	6	3	249	1	4.6061	0.3905
686	2013	9	9	3	252	1	4.3631	0.3499
687	2013	9	20	3	263	1	3.8177	0.4164
688	2013	9	20	3	263	1	3.8177	0.3788
689	2013	9	22	3	265	1	3.7735	0.3598
690	2004	6	13	2	165	2	0.0162	0.3044
691	2004	6	14	2	166	2	0.0191	0.2637
692	2004	6	22	2	174	2	0.0350	0.3197
693	2004	6	23	2	175	2	0.0357	0.2811
694	2004	6	25	2	177	2	0.0358	0.3144
695	2004	6	30	2	182	2	0.0399	0.2786
696	2004	7	4	2	186	2	0.0671	0.3044
697	2004	7	4	2	186	2	0.0671	0.3711
698	2004	7	18	2	200	2	0.5214	0.5293
699	2004	7	19	2	201	2	0.5687	0.4997
700	2004	7	20	2	202	2	0.6163	0.5225

701	2004	7	27	2	209	2	0.9465	0.5270
702	2004	7	27	2	209	2	0.9465	0.5890
703	2004	8	7	2	220	2	1.4564	0.6307
704	2004	8	8	2	221	2	1.5087	0.7195
705	2004	8	14	2	227	2	1.8821	0.7482
706	2004	8	21	2	234	2	2.4353	0.7317
707	2004	8	24	2	237	2	2.6709	0.7502
708	2004	8	29	2	242	2	3.0040	0.5785
709	2004	8	30	2	243	2	3.0577	0.7100
710	2004	9	6	2	250	2	3.2791	0.6456
711	2004	9	9	2	253	2	3.2756	0.6406
712	2004	9	13	2	257	2	3.1607	0.5307
713	2004	9	16	2	260	2	2.9822	0.5407
714	2004	9	25	2	269	2	2.0090	0.4044
715	2004	9	29	2	273	2	1.4560	0.4102
716	2006	5	25	2	145	2	0.0072	0.2067
717	2006	5	28	2	148	2	0.0172	0.2401
718	2006	6	6	2	157	2	0.0323	0.2623
719	2006	6	9	2	160	2	0.0373	0.2532
720	2006	6	13	2	164	2	0.0563	0.2775
721	2006	6	13	2	164	2	0.0563	0.2466
722	2006	6	20	2	171	2	0.1202	0.2801
723	2006	6	22	2	173	2	0.1378	0.2873
724	2006	7	1	2	182	2	0.2933	0.3443
725	2006	7	6	2	187	2	0.4755	0.4193
726	2006	7	6	2	187	2	0.4755	0.3373
727	2006	7	15	2	196	2	0.9590	0.5310
728	2006	7	17	2	198	2	1.0897	0.5608
729	2006	7	20	2	201	2	1.3065	0.5781
730	2006	7	26	2	207	2	1.8392	0.7345
731	2006	7	29	2	210	2	2.1366	0.7055
732	2006	8	4	2	216	2	2.6367	0.7375
733	2006	8	5	2	217	2	2.7114	0.7138
734	2006	8	9	2	221	2	3.0404	0.7654
735	2006	8	14	2	226	2	3.5170	0.8410
736	2006	8	14	2	226	2	3.5170	0.8564
737	2006	8	23	2	235	2	3.6697	0.7500
738	2006	8	29	2	241	2	3.4337	0.7156
739	2006	8	30	2	242	2	3.3925	0.6755
740	2006	9	12	2	255	2	2.8308	0.5726
741	2006	9	13	2	256	2	2.7785	0.4360
742	2006	9	17	2	260	2	2.5443	0.4331
743	2006	9	19	2	262	2	2.4093	0.4506
744	2006	9	24	2	267	2	2.0115	0.4025
745	2006	9	26	2	269	2	1.8316	0.3589
746	2006	10	1	2	274	2	1.3471	0.2848
747	2008	5	30	2	151	2	0.0128	0.2240
748	2008	6	6	2	158	2	0.0266	0.2553
749	2008	6	6	2	158	2	0.0266	0.2303
750	2008	6	13	2	165	2	0.0440	0.2327

751	2008	6	16	2	168	2	0.0647	0.2602
752	2008	6	20	2	172	2	0.0905	0.3076
753	2008	6	27	2	179	2	0.1233	0.3277
754	2008	7	2	2	184	2	0.2440	0.3018
755	2008	7	5	2	187	2	0.3517	0.4006
756	2008	7	10	2	192	2	0.4340	0.3939
757	2008	7	11	2	193	2	0.4330	0.4004
758	2008	7	15	2	197	2	0.4764	0.3915
759	2008	7	20	2	202	2	0.8040	0.4977
760	2008	7	22	2	204	2	1.0005	0.4997
761	2008	8	2	2	215	2	1.9237	0.6164
762	2008	8	3	2	216	2	1.9480	0.7016
763	2008	8	7	2	220	2	2.0672	0.7148
764	2008	8	7	2	220	2	2.0672	0.7371
765	2008	8	12	2	225	2	2.4633	0.7920
766	2008	8	23	2	236	2	3.0778	0.7330
767	2008	8	26	2	239	2	3.0645	0.6934
768	2008	9	1	2	245	2	3.1069	0.6354
769	2008	9	4	2	248	2	3.1869	0.5992
770	2008	9	17	2	261	2	3.1138	0.5101
771	2008	9	20	2	264	2	2.8151	0.3885
772	2008	9	26	2	270	2	1.8219	0.3212
773	2008	9	27	2	271	2	1.6234	0.2922
774	2004	6	14	3	166	2	0.0134	0.2933
775	2004	6	14	3	166	2	0.0134	0.2594
776	2004	6	23	3	175	2	0.0380	0.3301
777	2004	6	25	3	177	2	0.0448	0.3213
778	2004	7	4	3	186	2	0.1226	0.3559
779	2004	7	4	3	186	2	0.1226	0.3581
780	2004	7	12	3	194	2	0.3453	0.6006
781	2004	7	18	3	200	2	0.6065	0.4723
782	2004	7	19	3	201	2	0.6559	0.4548
783	2004	7	20	3	202	2	0.7070	0.5014
784	2004	7	27	3	209	2	1.1176	0.5328
785	2004	7	27	3	209	2	1.1176	0.5084
786	2004	8	7	3	220	2	1.8625	0.5756
787	2004	8	8	3	221	2	1.9122	0.7668
788	2004	8	14	3	227	2	2.0611	0.6124
789	2004	8	21	3	234	2	2.1907	0.6433
790	2004	8	24	3	237	2	2.3224	0.4894
791	2004	8	29	3	242	2	2.5749	0.6152
792	2004	8	30	3	243	2	2.6211	0.6369
793	2004	9	6	3	250	2	2.7796	0.6860
794	2004	9	9	3	253	2	2.7028	0.4600
795	2004	9	13	3	257	2	2.4156	0.5142
796	2004	9	16	3	260	2	2.0747	0.3410
797	2004	9	24	3	268	2	0.7721	0.3248
798	2004	9	25	3	269	2	0.5824	0.3250
799	2006	5	28	3	148	2	0.0111	0.3431
800	2006	6	6	3	157	2	0.0506	0.2366

801	2006	6	9	3	160	2	0.0669	0.2497
802	2006	6	13	3	164	2	0.0799	0.2746
803	2006	6	13	3	164	2	0.0799	0.2721
804	2006	6	20	3	171	2	0.1145	0.3145
805	2006	6	22	3	173	2	0.1598	0.3373
806	2006	6	29	3	180	2	0.3795	0.3028
807	2006	7	1	3	182	2	0.4089	0.3220
808	2006	7	6	3	187	2	0.4707	0.4238
809	2006	7	6	3	187	2	0.4707	0.3264
810	2006	7	15	3	196	2	1.1710	0.5050
811	2006	7	17	3	198	2	1.3643	0.5042
812	2006	7	20	3	201	2	1.5198	0.5366
813	2006	7	26	3	207	2	1.7565	0.5846
814	2006	7	29	3	210	2	2.0207	0.5602
815	2006	8	4	3	216	2	2.5559	0.6355
816	2006	8	5	3	217	2	2.6215	0.6253
817	2006	8	9	3	221	2	2.8070	0.7757
818	2006	8	14	3	226	2	2.8771	0.8251
819	2006	8	14	3	226	2	2.8771	0.5998
820	2006	8	23	3	235	2	2.8740	0.8396
821	2006	8	30	3	242	2	2.8026	0.7065
822	2006	9	12	3	255	2	2.3503	0.5755
823	2006	9	13	3	256	2	2.3027	0.5311
824	2006	9	17	3	260	2	2.1021	0.4783
825	2006	9	19	3	262	2	1.9975	0.4769
826	2006	9	24	3	267	2	1.7283	0.3974
827	2006	9	26	3	269	2	1.6180	0.4000
828	2006	10	1	3	274	2	1.3374	0.3232
829	2006	10	7	3	280	2	0.9947	0.3019
830	2008	5	30	3	151	2	0.0098	0.2384
831	2008	5	31	3	152	2	0.0123	0.2631
832	2008	6	6	3	158	2	0.0273	0.2600
833	2008	6	6	3	158	2	0.0273	0.3786
834	2008	6	13	3	165	2	0.0458	0.2697
835	2008	6	16	3	168	2	0.0591	0.2736
836	2008	6	20	3	172	2	0.0944	0.2451
837	2008	6	27	3	179	2	0.1602	0.3592
838	2008	7	2	3	184	2	0.2069	0.3006
839	2008	7	5	3	187	2	0.2706	0.4011
840	2008	7	10	3	192	2	0.4728	0.3814
841	2008	7	11	3	193	2	0.5089	0.3924
842	2008	7	15	3	197	2	0.4885	0.4045
843	2008	7	20	3	202	2	0.2960	0.4536
844	2008	7	22	3	204	2	0.4258	0.5591
845	2008	8	2	3	215	2	0.8138	0.5241
846	2008	8	3	3	216	2	0.7651	0.7256
847	2008	8	7	3	220	2	1.1968	0.7963
848	2008	8	7	3	220	2	1.1968	0.7722
849	2008	8	12	3	225	2	2.1793	0.8285
850	2008	8	16	3	229	2	2.4206	0.6117

851	2008	8	23	3	236	2	2.5001	0.6076
852	2008	9	1	3	245	2	2.8020	0.5683
853	2008	9	4	3	248	2	2.8931	0.5095
854	2008	9	17	3	261	2	2.5105	0.4559
855	2008	9	20	3	264	2	2.0774	0.3826
856	2010	5	28	3	148	2	0.0006	0.3465
857	2010	6	17	3	168	2	0.0589	0.3070
858	2010	6	21	3	172	2	0.0926	0.3478
859	2010	6	22	3	173	2	0.1027	0.2775
860	2010	6	26	3	177	2	0.1503	0.2703
861	2010	7	1	3	182	2	0.2250	0.3654
862	2010	7	6	3	187	2	0.3247	0.4275
863	2010	7	10	3	191	2	0.4411	0.3843
864	2010	7	14	3	195	2	0.5975	0.4626
865	2010	7	19	3	200	2	0.8444	0.5100
866	2010	7	27	3	208	2	1.3663	0.5716
867	2010	7	27	3	208	2	1.3663	0.5601
868	2010	7	31	3	212	2	1.7395	0.5261
869	2010	8	3	3	215	2	2.0382	0.6299
870	2010	8	8	3	220	2	2.3554	0.5602
871	2010	8	11	3	223	2	2.4110	0.5355
872	2010	8	15	3	227	2	2.4600	0.7649
873	2010	8	20	3	232	2	2.5629	0.5806
874	2010	8	22	3	234	2	2.6078	0.6878
875	2010	8	25	3	237	2	2.6685	0.6405
876	2010	8	29	3	241	2	2.7191	0.5513
877	2010	9	3	3	246	2	2.6955	0.7540
878	2010	9	7	3	250	2	2.5807	0.6091
879	2010	9	12	3	255	2	2.3260	0.6074
880	2010	9	14	3	257	2	2.1949	0.5725
881	2010	9	26	3	269	2	1.1684	0.3523
882	2010	9	28	3	271	2	0.9729	0.3262
883	2010	9	30	3	273	2	0.7750	0.3600
884	2012	5	28	3	149	2	0.0167	0.2216
885	2012	5	28	3	149	2	0.0167	0.2652
886	2012	6	4	3	156	2	0.0338	0.2726
887	2012	6	18	3	170	2	0.1359	0.2712
888	2012	6	24	3	176	2	0.3313	0.2626
889	2012	6	26	3	178	2	0.4225	0.3053
890	2012	6	27	3	179	2	0.4563	0.3302
891	2012	7	6	3	188	2	0.3472	0.4139
892	2012	7	10	3	192	2	0.4710	0.4006
893	2012	7	17	3	199	2	1.0977	0.4480
894	2012	7	22	3	204	2	1.2049	0.4651
895	2012	7	29	3	211	2	1.3682	0.4266
896	2012	8	4	3	217	2	1.5034	0.5105
897	2012	8	5	3	218	2	1.5148	0.3278
898	2012	8	15	3	228	2	1.7589	0.4280
899	2012	8	21	3	234	2	2.0125	0.4507
900	2012	8	27	3	240	2	2.2198	0.4436
901	2012	8	29	3	242	2	2.2569	0.3771
902	2012	8	30	3	243	2	2.2668	0.3124
903	2012	9	5	3	249	2	2.1688	0.3280
904	2012	9	8	3	252	2	2.0045	0.3427
905	2012	9	15	3	259	2	1.4007	0.2541
906	2012	9	19	3	263	2	0.9777	0.2671

Table S2.2: Summary of observed standing wet biomass and MODIS derived *GrWDRVI* for each of the 3 fields near Mead, NE.